ION DIAGNOSTICS FOR HIGH-INTENSITY LASER-MATTER INTERACTION EXPERIMENTS.

Prof. Claudio Verona

Università di Roma Tor Vergata
DIPARTIMENTO DI INGEGNERIA INDUSTRIALE

21th SEMINAR ON SOFTWARE FOR NUCLEAR, SUBNUCLEAR AND APPLIED PHYSICS

09–14 giu 2024
Hotel Porto Conte, Alghero

LASER-DRIVEN ION ACCELERATION

Energy: from few mJ up to hundreds of J

Pulse duration: from tens of fs (“short pulse ”) up to ns (“long pulse”)

Focal spot size: from few up to tens of μm

For Laser intensities higher than 10^{18} W/cm^2 several laser-driven acceleration mechanism can occur

$$I\left(\frac{W}{cm^2}\right) \approx 1.33 \cdot 10^{-3} E^2 \left(\frac{V}{cm}\right)^2$$

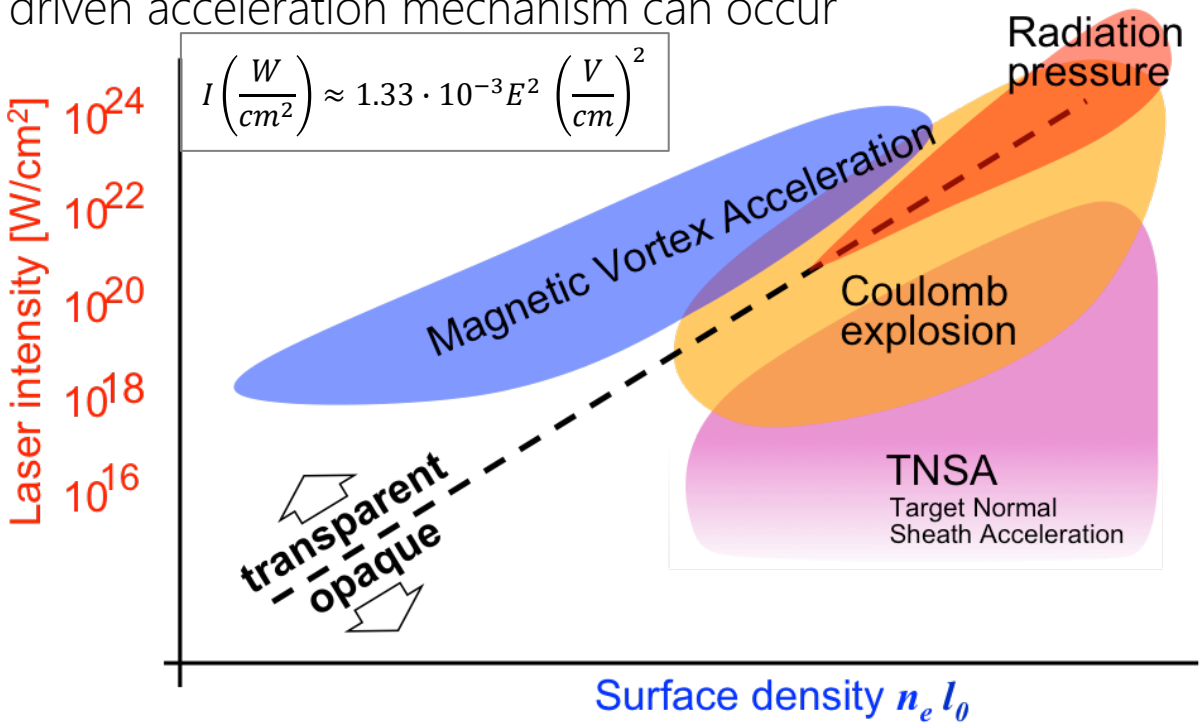

TNSA
Laser: Low Intensity
Target: Thick solid density foils
Ion Energy: ~100 MeV

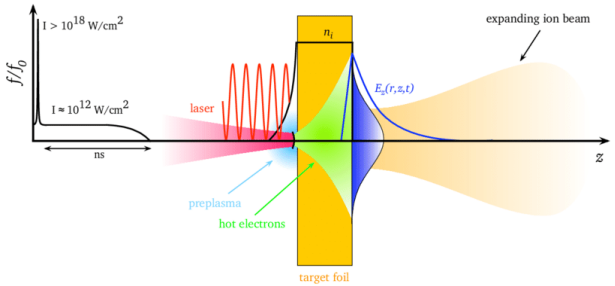

Coulomb explosion
Laser: High Intensity/ large focal spot
Target: Thin solid density foils
Ion Energy: hundreds of MeV

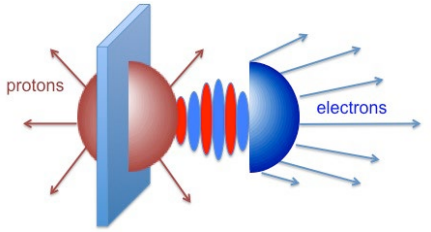

Radiation pressure acceleration (RPA)
Laser: Very High Intensity
Target: Thin solid density foils
Ion Energy: hundreds of MeV

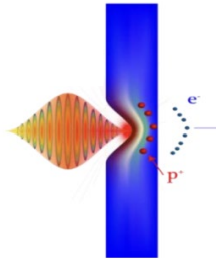

Energy spectrum of ion changes according to the interaction condition:

- ✓ Laser energy and intensity
- ✓ Target type
- ✓ Focal spot

ION DIAGNOSTICS

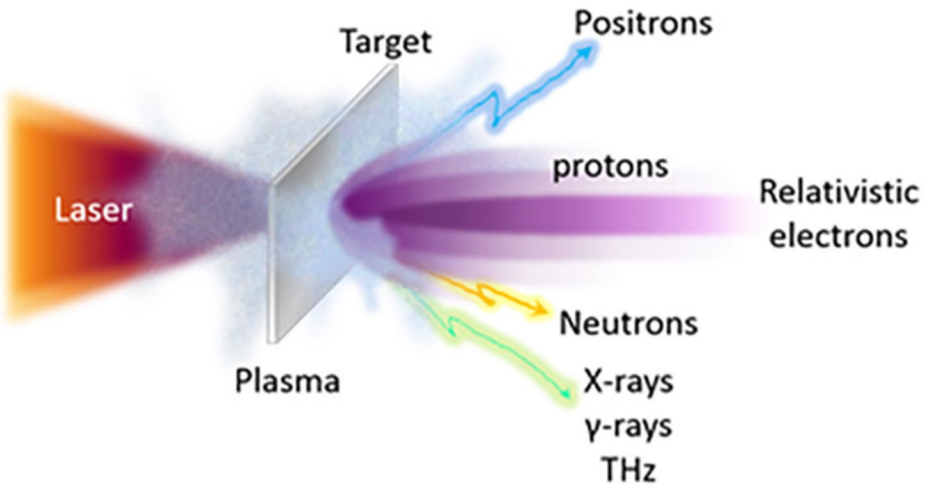

Laser-generated plasma emission:

- Protons
- Multi ion species
- X-rays and electrons
- Neutrons
- Electromagnetic pulse (EMP)

- Challenges for detection further arise from the harsh plasma environment.
- Experimental setups generally incorporate a combination of complementary devices featuring various detection principles, online and offline analysis and acceptance angles.

The ideal diagnostic system should have:

- High sensitivity
- High energy resolution

and should allow to retrieve:

- Spectrum of accelerated ions
- Angular distribution of accelerated ions
- Particle discrimination

but it also has to provide:

- Electro Magnetic Pulses (EMPs) robustness
- Real-time detection (in particular for high repetition rate lase)

ION DIAGNOSTICS

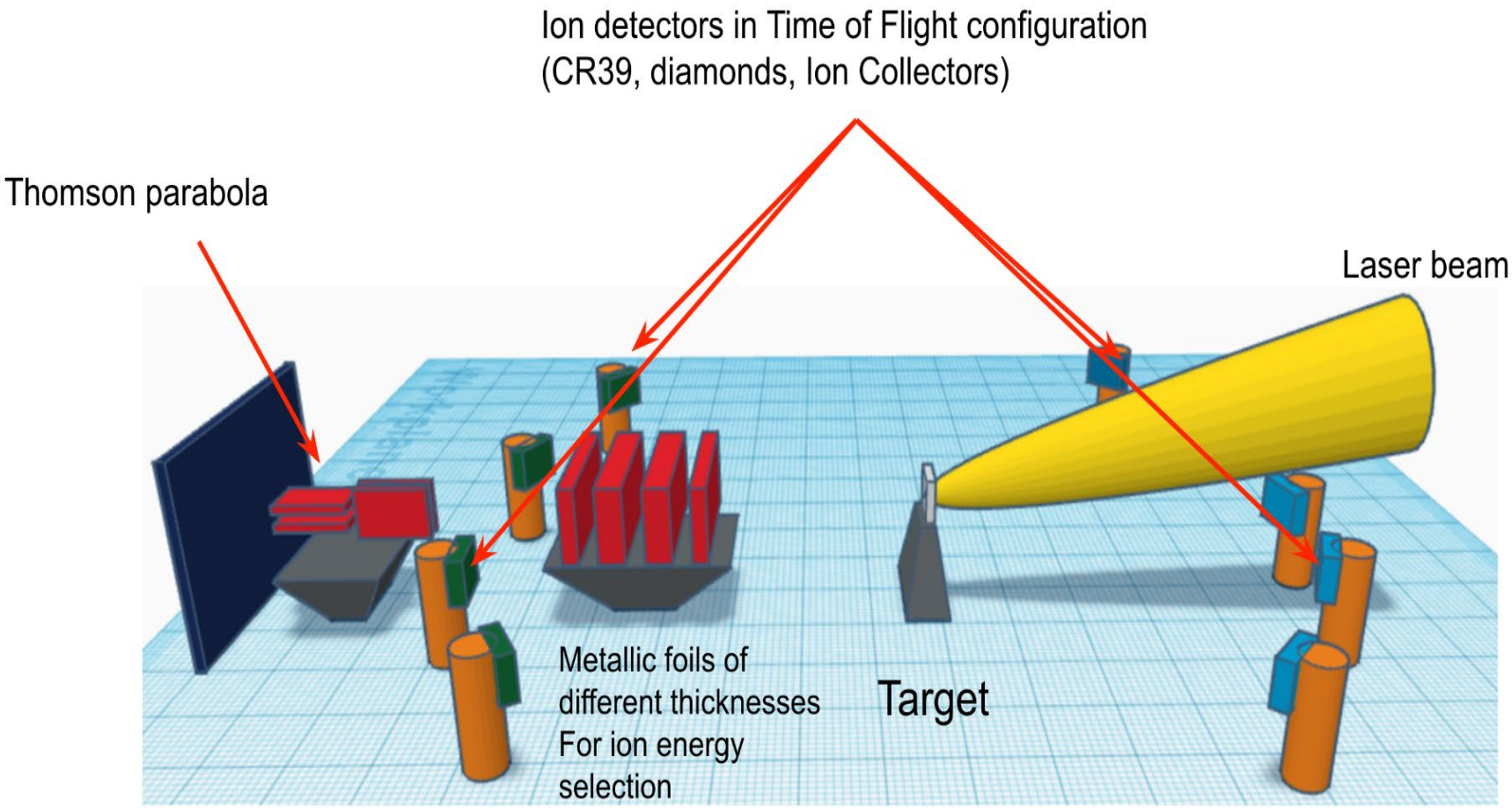

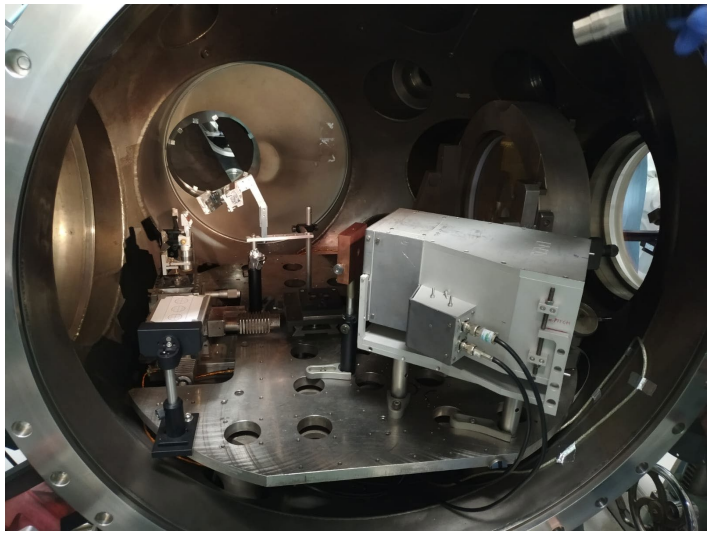

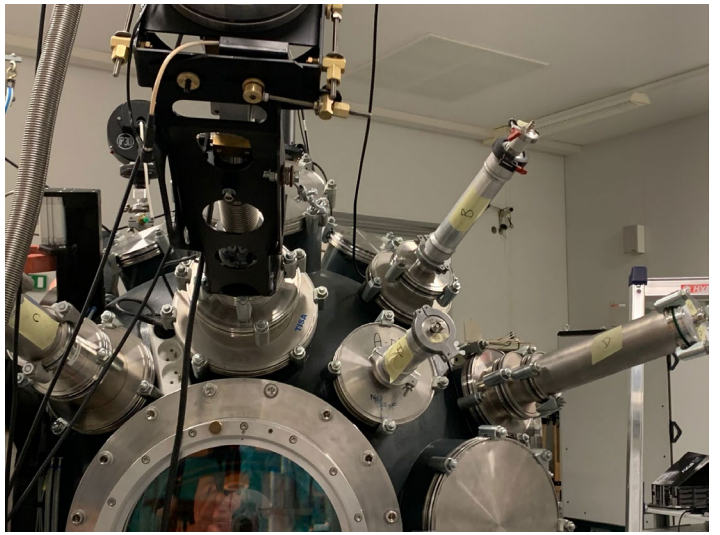

Solid state track detectors

SOLID STATE TRACK DETECTOR

- Solid state nuclear track detectors (SSNTDs) such as CR39 polymer and PM-355 plastic, are used to detect particles by observing their track inside the detector material.

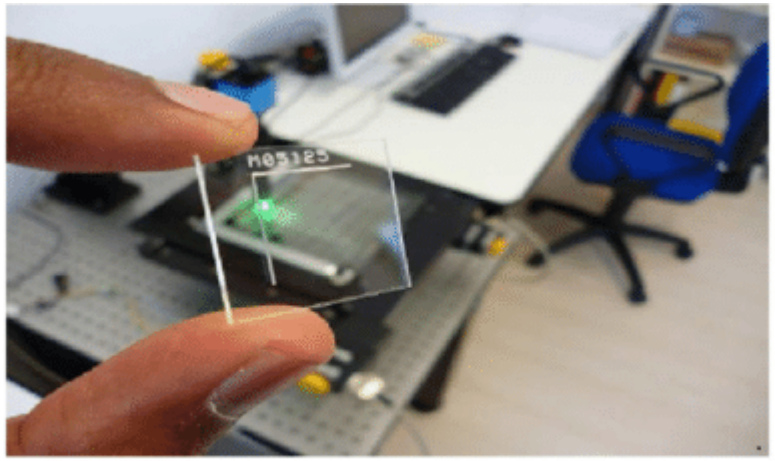

(a) A View of CR-39 detector

- In general, CR39 is sensitive to protons of energy ≤ 14 MeV, alpha particles of energy ≤ 100 MeV, and heavy ions of all energies. Neutrons of energy between 500 keV and 20 MeV can be detected via an enlarged latent damage trail, or "track," from recoil protons formed as a result of interactions between neutrons and the hydrogen nuclei of the detector. Electrons, X-rays, and γ-rays do not produce a remarkable effect on the detector but change its average solubility.

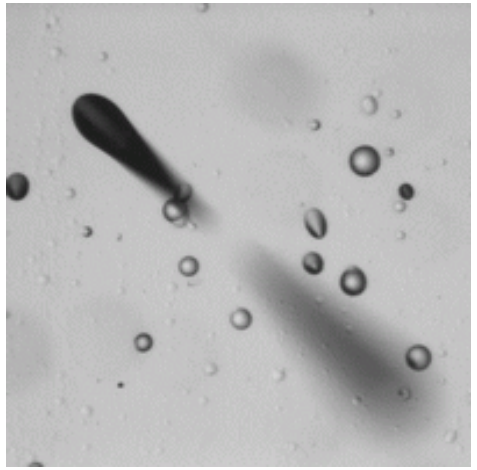

- A particle striking the SSNTD deposits its energy by creating a proportional damage trail, referred to as a latent track along the particle's trajectory, as it penetrates the detector. The geometry of this track (size, shape and depth) depends on the incidence angle, energy and LET of the incident particle.

SOLID STATE TRACK DETECTOR

- The latent track is too small (few nanometers) to be observed optically but can be enlarged through chemical wet etching in a highly alkaline solution (i.e. NaoH).
- Etching dissolves the polymer to the point where the track opening is large enough (few micrometers). The etching solution preferentially attacks the latent damage trail, leaving a conical pit at the intersection of the particle's trajectory and the detector surface. The dimensions of the elliptical opening of the conical track are proportional to the LET of the charged particle that created the latent damage trail.
- The etched CR39 is then read-out using a dedicated automatic high-resolution optical microscope.
- SSNTD requires careful pit analysis, e.g., via numerical image processing of microscope data.

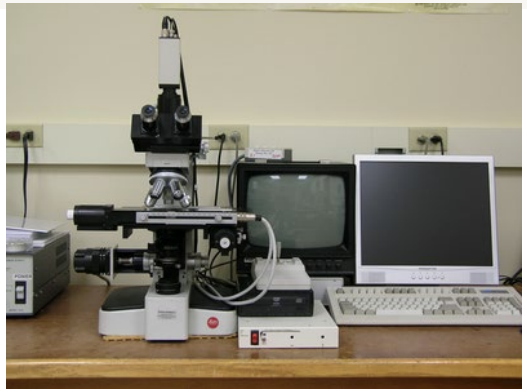

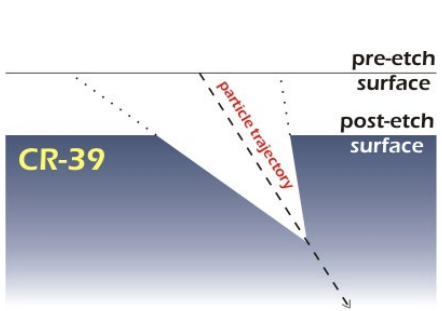

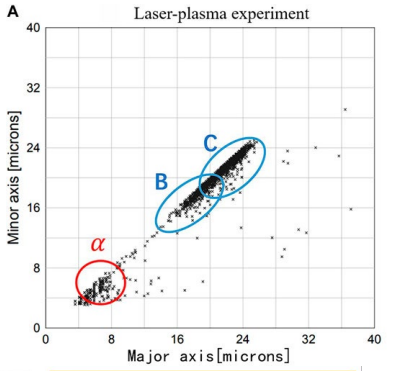

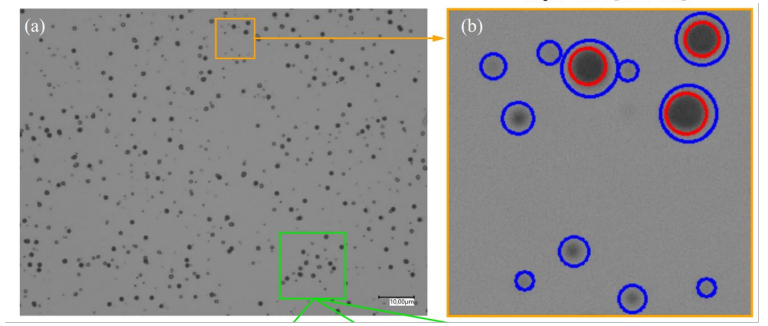

SOLID STATE TRACK DETECTOR

- The etching process depends on several parameters such as etching time, temperature, concentration and inherent purity of NaOH solution, which can differ from one experiment to the other and material from the same manufacturer, resulting in different characteristics of the tracks.

- The reproducibility of the detector parameters affects largely the detector response.

- Larger times of etching should be needed but the relation is no more univocal in the whole energy range.
  The same particle of different energies might produce a pit of the same size.

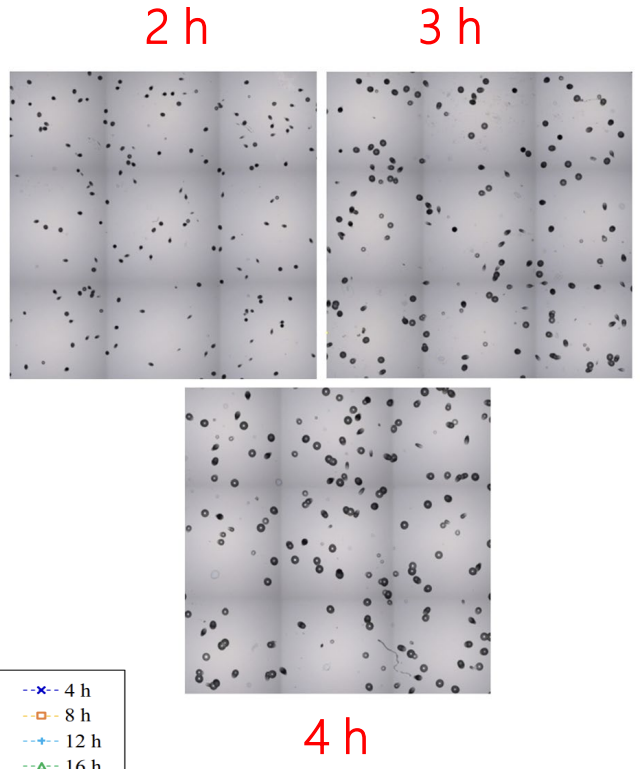

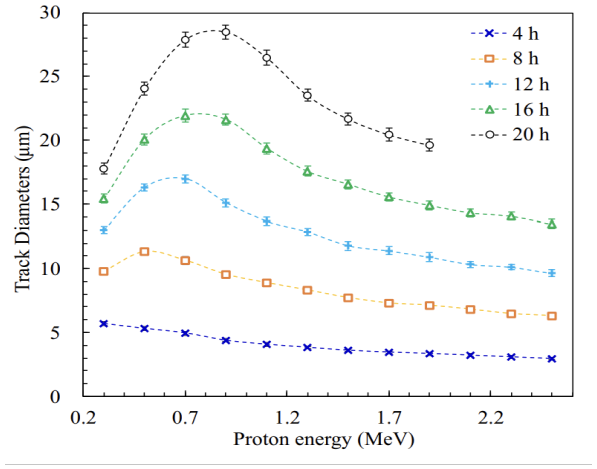

SOLID STATE TRACK DETECTOR

- Calibration of SSNTD: exposure of the detector to known ion beams and the examination of the resulting tracks under different conditions of etching solution, temperature and time. The calibration intends to establish a relationship between the track diameter and the energy of the impinging particles.
- Information on particle energy can be inferred by track dimension and etching rate, compared with that of the detector bulk. Information on the particle type may be achieved.
- On the calibration curve, one diameter may correspond to two particle energies. In this case, the gray level and the depth of track can be used to distinguish which energy is the correct one: on the low-energy side, the track is shallow, and the gray level is lower while on the high-energy side the track reaches a bigger value on the gray scale.

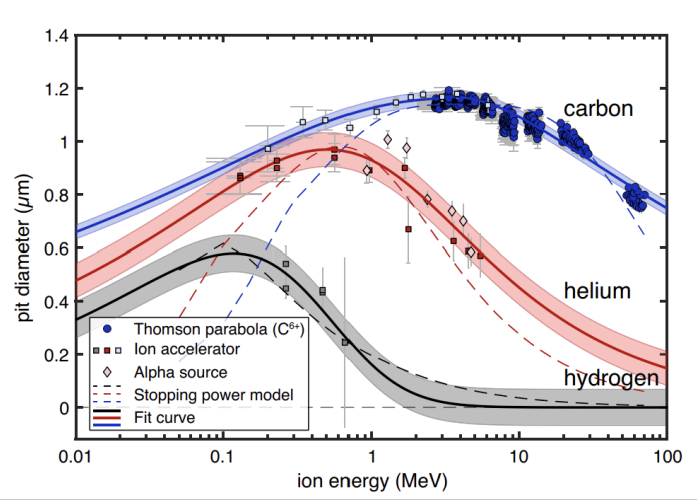

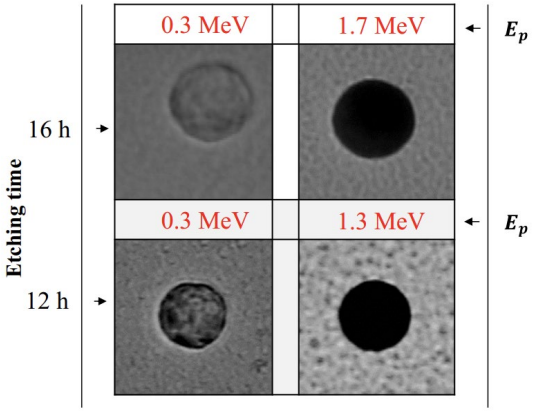

SOLID STATE TRACK DETECTOR

- The most common method to distinguish the particles' energy is the "Range-Filter Method"

➢ It is possible to use plastic or metal foils as filters, capable of stopping low-energy and heavy particles (for example Carbon, Silicon) and leave high-energy particles (e.g. protons) to pass through them.

➢ The use of filters decreases the energy of particles reaching the detector and may cut most of the particle spectrum.

- It is useful to put some filters on the surface of the CR-39 to optimize the detection avoiding the saturation from the low energy component.

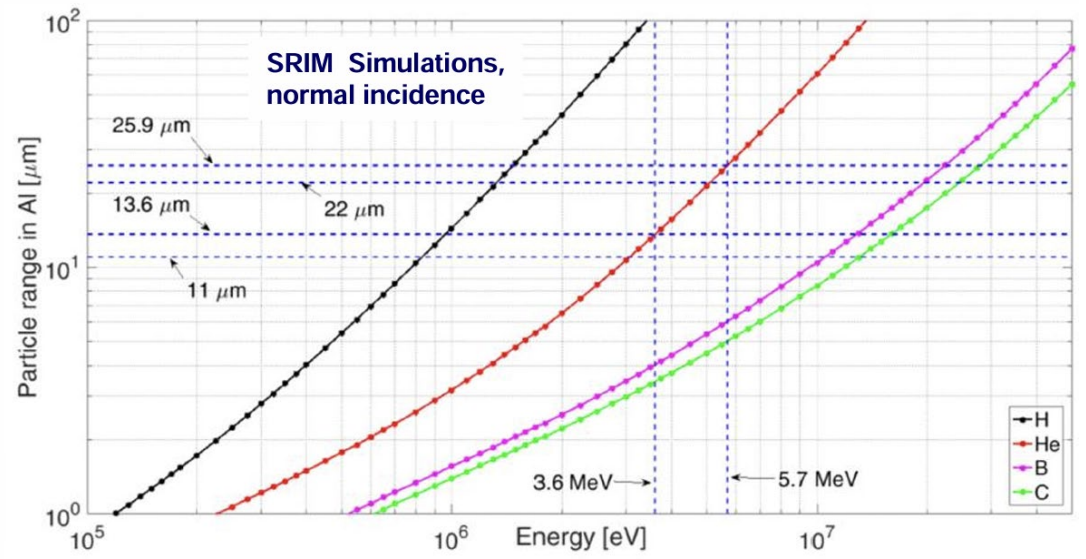

SOLID STATE TRACK DETECTOR

- Energetic spectrum of particles reconstruction

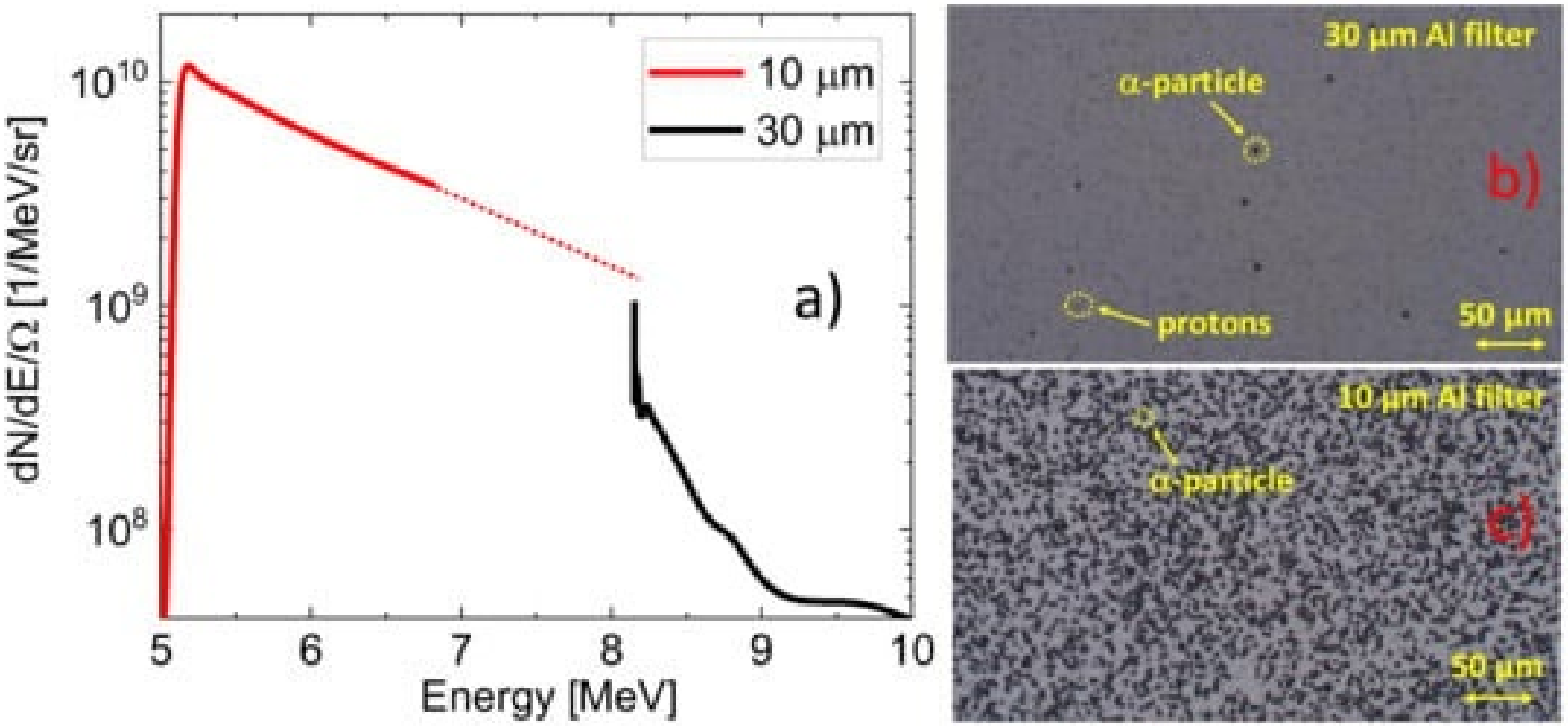

SOLID STATE TRACK DETECTOR

Solid State Nuclear Track Detector (SSNTD)

- Passive detector
- Time consuming (post processing & calibration)
- Strong background

- Small dimensions
- Insensitivity to electromagnetic radiation
- Ion discrimination
- Energy Spectrum reconstruction

Thomson spectrometer

THOMSON SPECTROMETER

- Thomson Parabola (TP) spectrometers are well-known effective detectors used for discriminating ions with different $\frac{A}{Z}$ ratio in high power laser experiments.
- An electrostatic and a magnetostatic field, both orthogonal to the incoming particle beam direction, determine a deflection of the particles leading to parabolic traces, each univocally corresponds to one particle charge to mass ratio $\left(\frac{A}{Z}\right)$ and the shape is also fixed by the TP geometry.
- The zero point of the parabola represents the non-deflected particles (x-rays) generated by the interaction and passing through the detector without any influence due to the electric and magnetic field and passing through the pinhole.

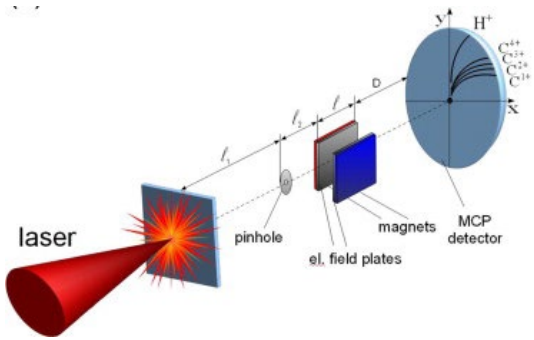

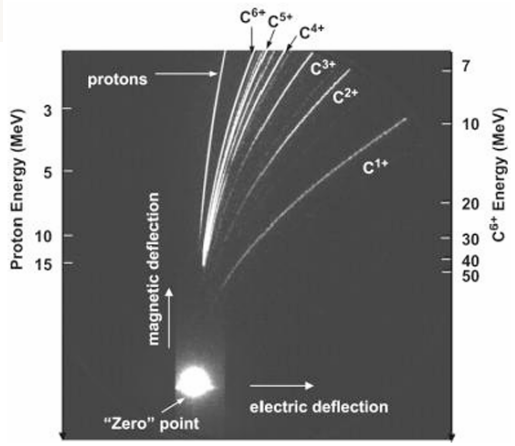

the x and y coordinates of the trace can be derived from the Lorentz equation

$$\begin{cases} x = \dfrac{qB_0 l_B\left(\frac{l_B}{2} + D_B\right)}{mv} \\ y = \dfrac{qE_0 l_E\left(\frac{l_E}{2} + D_E\right)}{mv^2} \end{cases}$$

Combining the two equation, the parabola equation is

$$y = \frac{m}{q}\frac{E_0 l_E\left(\frac{l_E}{2} + D_E\right)}{\left[B_0 l_B\left(\frac{l_B}{2} + D_B\right)\right]^2}x^2$$

THOMSON SPECTROMETER

- TP parameters (deflecting fields) affect data acquisition. Indeed, high electric and magnetic fields are necessary for a suitable trace separation at high energies.
- Size and shape of the pinhole must be carefully selected to find the best compromise between resolution (dependent on solid angle Ω) and sensitivity as well as the X-ray noise.
- Large pinholes enhance sensitivity but reduce spectral resolution and determine larger parabola widths $S_t \sim \left(1 + \frac{D_2}{D_1}\right) d_{pinhole}$
- The enhancement of the sensitivity implies larger background noise that can be coupled with the spectrometer (EMP and X-ray inside the spectrometer).

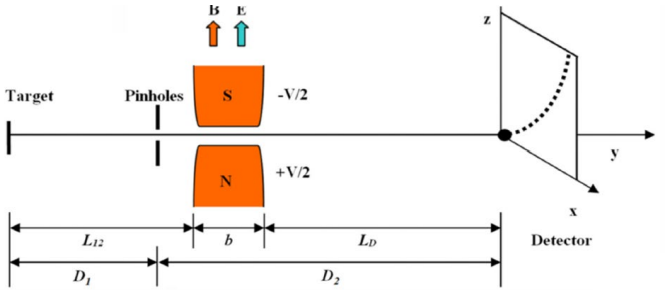

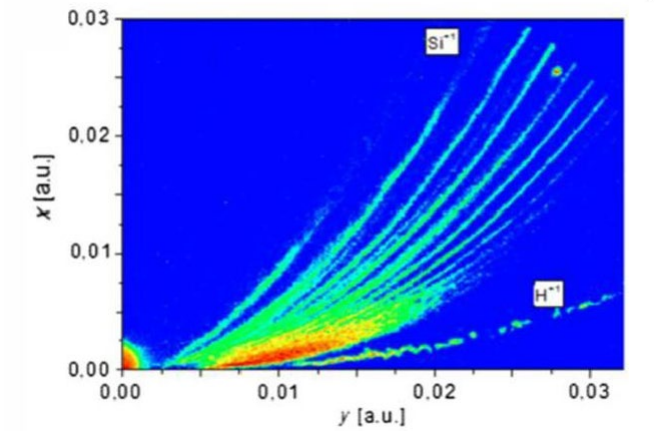

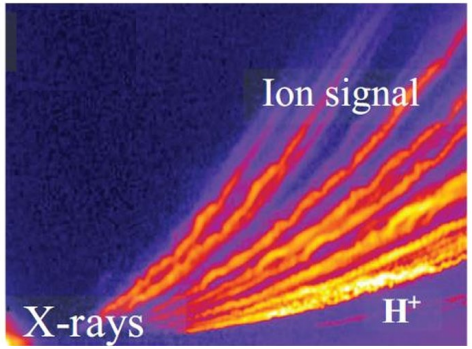

THOMSON SPECTROMETER

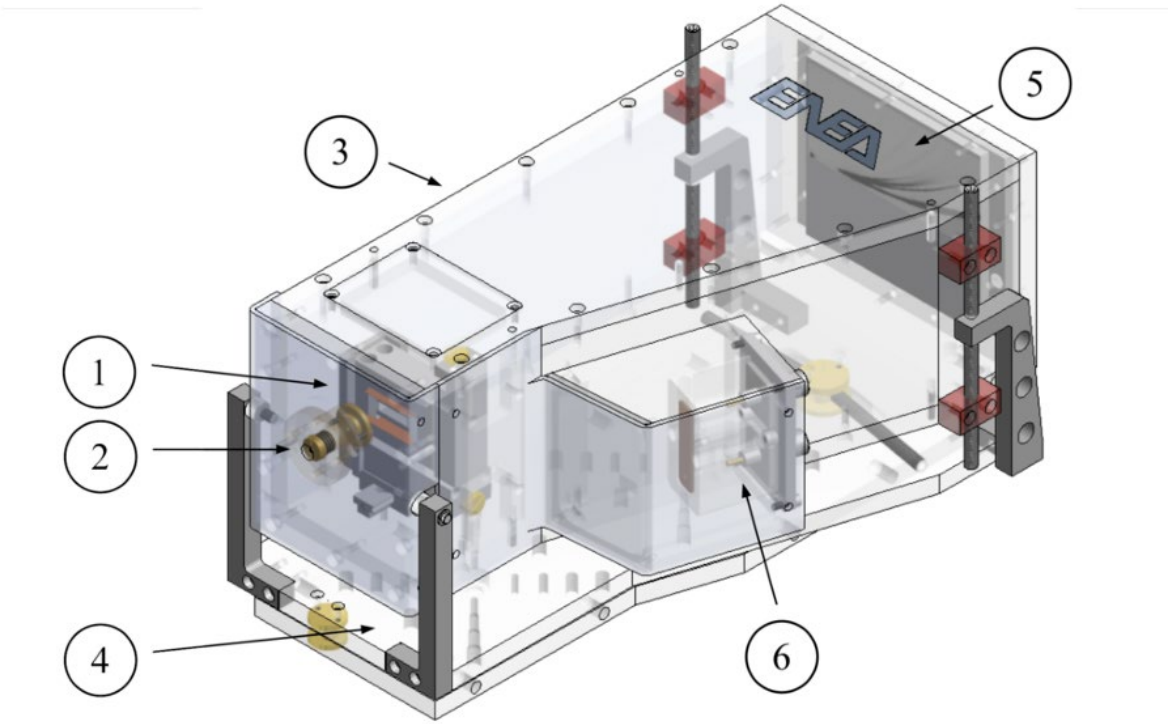

1. The deflecting-field assembly.
2. The two-pinhole assembly.
3. The external casing.
4. The tilt-and-yaw adjustments support.
5. The detector and alignment laser supports.
6. The high voltage connectors.

THOMSON SPECTROMETER

- Most used detectors are CCD screen with a micro channel plate (MCP) or image plate detectors as well as scintillators. Using calibrated detectors, it is possible to retrieve the absolute particle energetic spectrum.
- An image is acquired with the TP and the recorded traces are overlapped with the corresponding parabolas. To every point of the parabola is assigned a velocity value which is converted into a kinetic energy value.
- The intensity value on the imaging plane is calibrated to a particle number so that reading out the intensity along the parabola with energy assigned to every point yields the energy spectrum for a particular particle specie.

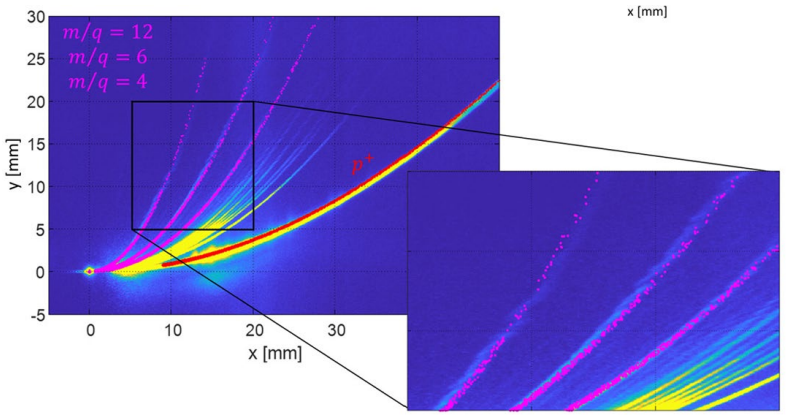

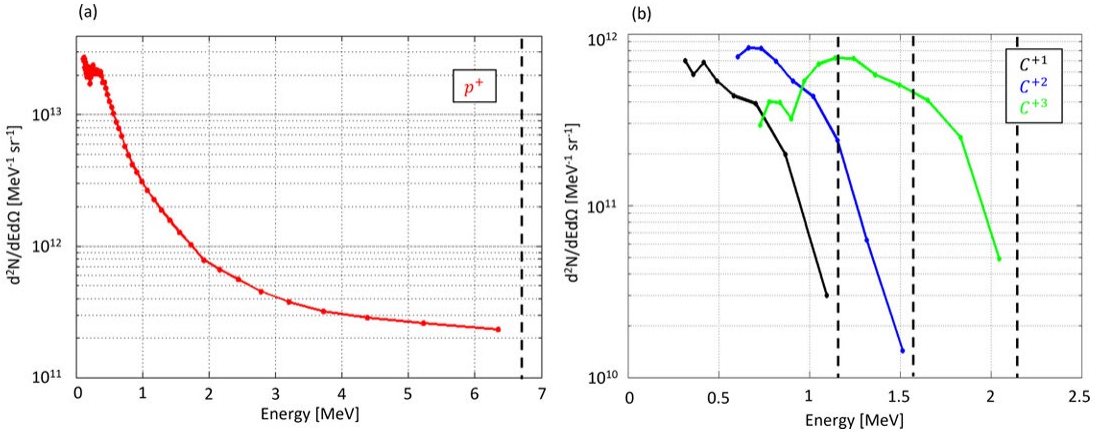

THOMSON SPECTROMETER

- The parabolic traces of ion species with the same Z/A will overlap at the detector plane, preventing their spectra to be characterised. Ex: to detect the lightest of the overlapping ion species, foil filters in front of the detector, which would preferentially stop heavier ions and allow only lighter species to be detected. A solution may be to use SSNTD as detectors in Thomson Spectrometers. The techniques described for particle discrimination can give some help.

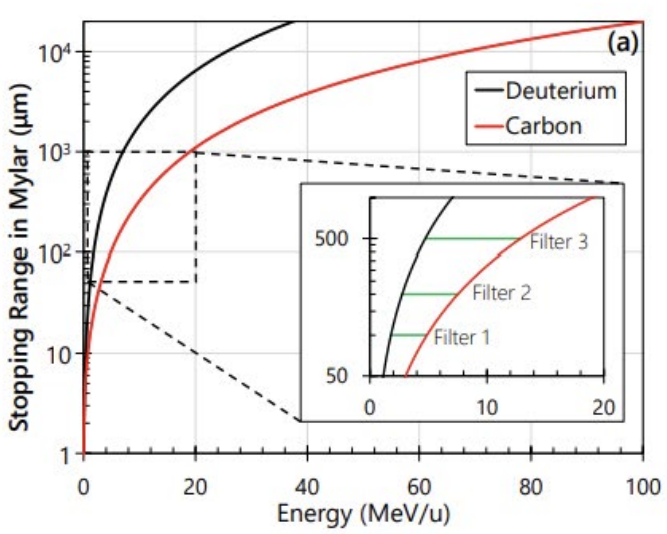

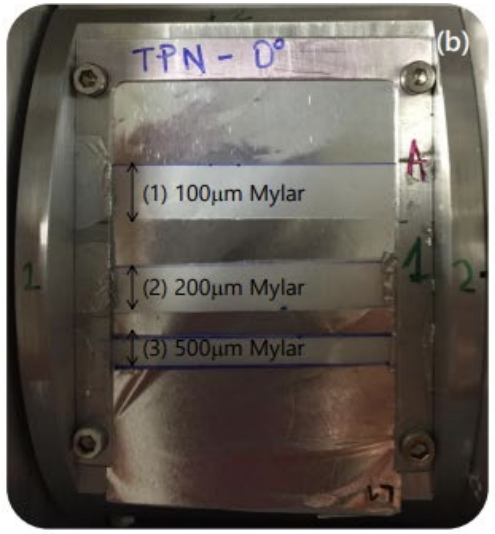

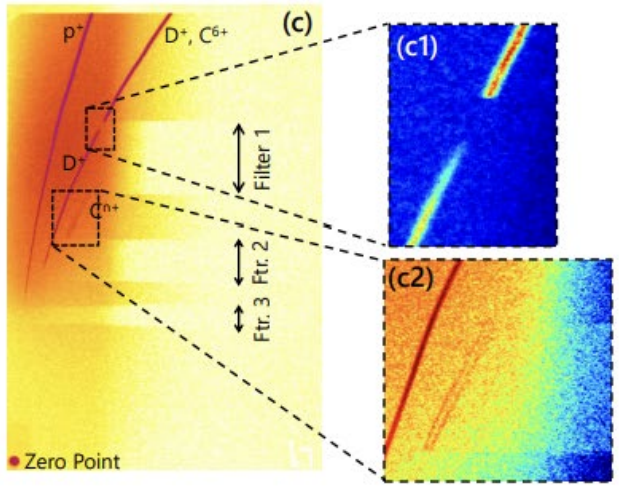

THOMSON SPECTROMETER

Thomson spectrometers (TS)

- Ion trace overlaps with fully stripped ions (the same Z/A)
- Sensitive to EMP and X-ray radiation noise
- High voltage operation

- Active detector
- Ion discrimination according to mass-to-charge ratio
- Energetic spectrum reconstruction

A. Alejo et al, Journal of Instrumentation, 11, C10005 (2016)

Charge particle activation analysis

ACTIVATION ANALYSIS OF CHARGE PARTICLES

- Charged particle activation analysis (CPAA) is based on charged particle (CP) induced nuclear reactions producing radionuclides, that are identified and quantified by their characteristic decay radiation.
- CPAA is based on a nuclear reaction

$$A(a,b)B \quad (Q-value >< 0)$$

where A is the stable target nuclide (at rest), ``a'' is a CP, B is a radionuclide, ``b'' is the particle(s) or photon emitted.

- Two important characteristics are the minimum CP energy required to induce such a nuclear reaction, and the probability that this reaction will proceed.
- The probability of a nuclear reaction is expressed as the cross-section (barn). The cross-section for a particular nuclear reaction depends on the energy of the CP. It is zero for CPs below the threshold energy of that reaction. For CP energies exceeding the threshold energy and Coulomb barrier, the cross-section increases up to a maximum (typically 1 barn).
- The first step is to make an appropriate choice for nuclear reaction on the basis of which particle is expected to be detected.

ACTIVATION ANALYSIS OF CHARGE PARTICLES

The interaction of protons and ^{56}Fe can generate neutrons

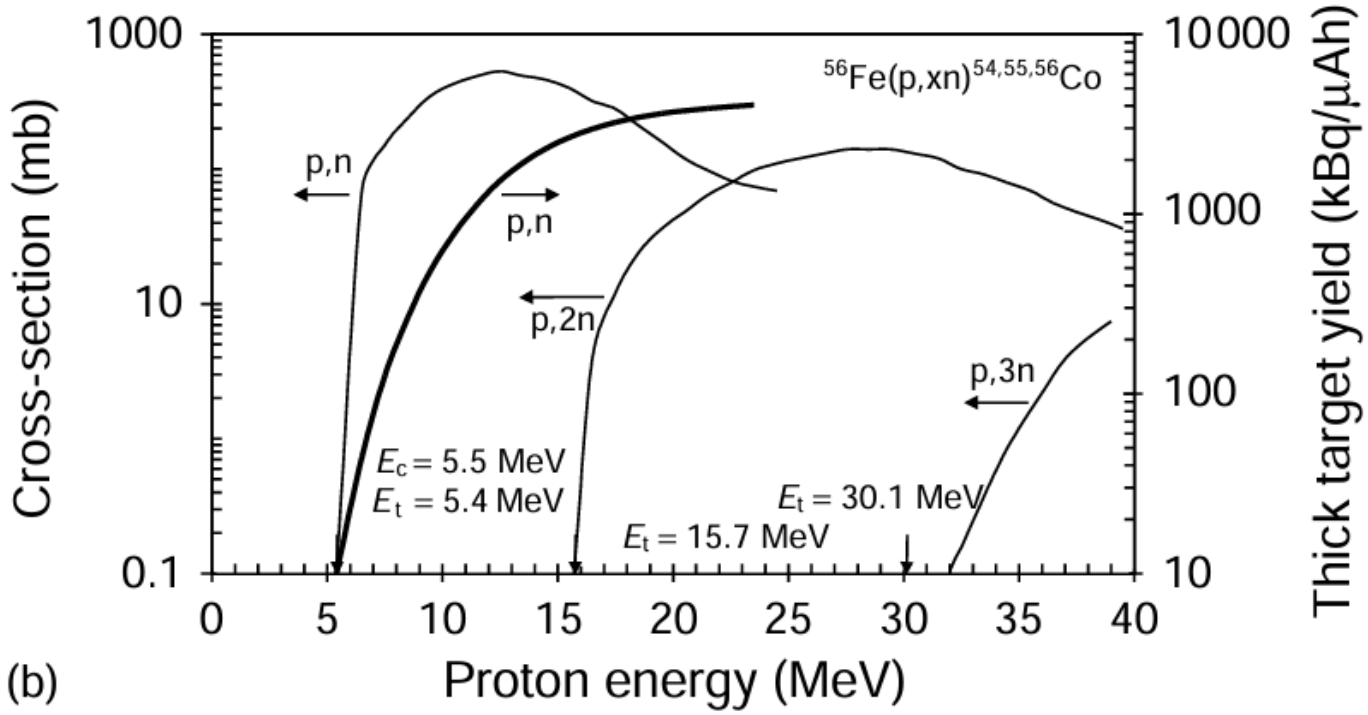

$$^{56}Fe(p,n)^{56}Co$$

The threshold energy of this reaction is 5.4 MeV. The cross-section increase to a maximum at 13 MeV.

$$^{56}Fe(p,2n)^{55}Co$$

The threshold energy of this reaction is 15.7 MeV. The cross-section increase to a maximum at 25-30 MeV.

$$^{56}Fe(p,3n)^{54}Co$$

The threshold energy of this reaction is 32 MeV.

ACTIVATION ANALYSIS OF CHARGE PARTICLES

TABLE I. Expected reaction rates N (corrected by concentration) using Eq. (2) and assuming $\int b(\Omega)d\Omega = 1/5$. The E_γ column refers to the highest intensity γ ray emitted by the isotope; $T_{1/2}$ is the half-life.[12]

No.	Reaction	Target	Thickness (mm)	N (10^8)	Q (MeV)	E_γ (keV)	$T_{1/2}$
1	^{63}Cu(p,n)^{63}Zn	^{nat}Cu	1	1.4	−4.15	511	38.5 min
2	^{63}Cu(p,n)^{63}Zn	^{63}Cu	0.011	0.11	−4.15	511	38.5 min
3	^{70}Zn(p,4n)^{67}Ga	^{70}Zn	0.032	1.8×10^{-3}	−27.68	93.3	3.26 d
4	^{70}Zn(p,α)^{67}Cu	^{70}Zn	0.032	2.6×10^{-3}	2.62	185	2.57 d
5	^{10}B(p,α)^{7}Be	^{nat}B	2	0.28	1.15	477.6	53.2 d
6	^{11}B(p,n)^{11}C	^{nat}B	2	1.4	−2.76	511	20.4 min
7	^{11}B(p,α)^{8}Be	^{nat}B	2	2.2	8.6	⋯	$8\ 10^{-17}$ s
8	^{12}C (p,X)^{11}C	CR39	1	0.1	−16.5	511	20.4 min
9	^{12}C(p,p)3α	CR39	1	0.88	−7.27	⋯	⋯
10	^{63}Cu(α,X)^{65}Zn	^{nat}Cu	1	⋯	−10.4	1115.5	244 d
11	^{65}Cu(α,X)^{68}Ga	^{nat}Cu	1	⋯	−5.8	511	67.7 min
12	^{18}O(p,n)^{18}F	^{nat}B (^{18}O 8.7×10^{-5}%)	2	3	−2.44	511	109.7 min

Interesting nuclear reaction used in proton boron fusion pB experiments (boron target).

$$^{10}B(p,\alpha)\ ^{7}Be \qquad Q>0$$

The released radioactive ^{7}Be decays emitting 477keV γ-rays.

$^{10}B(p,\gamma)^{11}C$ (Q<0, Energy protons above ~1MeV)

The released radioactive ^{11}C and γ-emission at 512keV can be an important observable.

$^{11}B(p,n)^{11}C$ (Q<0, Energy protons above ~3MeV)

The interaction of protons and ^{11}B can generate neutrons.

ACTIVATION ANALYSIS OF CHARGE PARTICLES

- Measurements of irradiated samples are done by γ-spectrometry or positron counting. Time management is important to improve signal-to-noise ratio (and thus the detection limit and repeatability).
- γ -spectrometry can be performed by a Germanium semiconductor detector (liquid nitrogen cooled). One γ -ray interacts with the detector by Compton scattering or the photoelectric effect. The photo- or Compton electron formed causes ionization in the detector and many electron-hole pairs are formed. The generated charge is proportional to the γ -energy.
- After linear amplification and analog-to digital conversion (ADC), the multi-channel analyzer shows a digital spectrum with peak(s) corresponding to the γ -energy/energies, and, at the lower energy side, a Compton continuum.

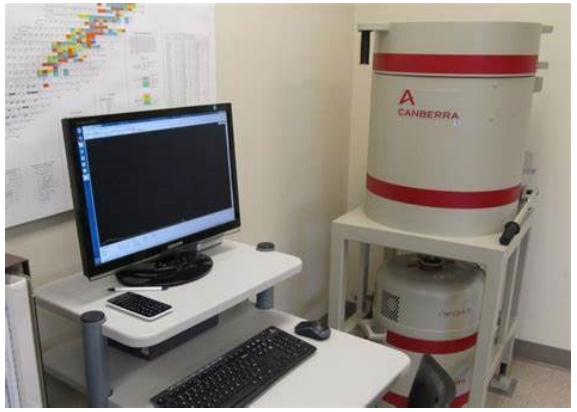

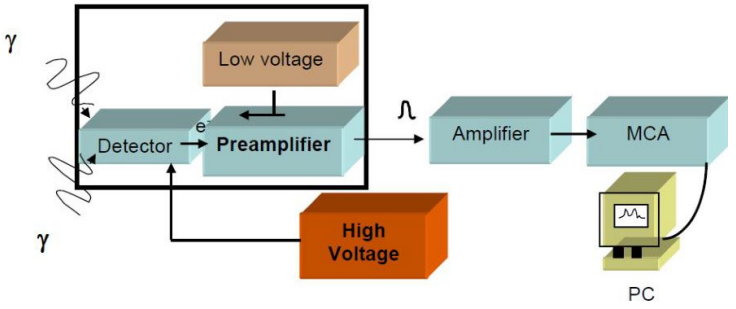

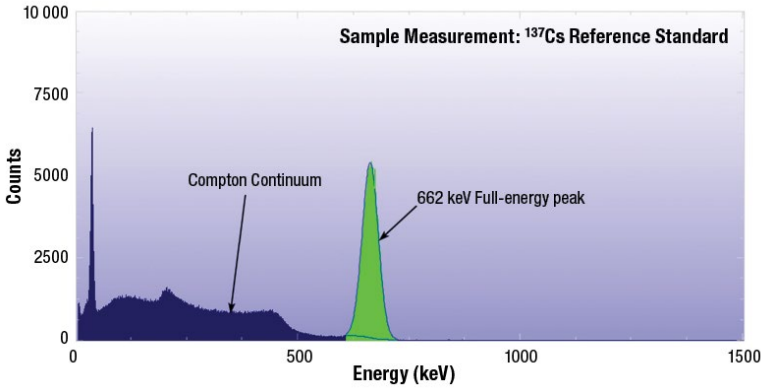

ACTIVATION ANALYSIS OF CHARGE PARTICLES

CPAA technique

- inherent complexity
- Expensive (reading set-up)
- passive technique

- Low detection limit
- Outstanding accuracy
- Absolute response

Time of Flight detectors

TIME OF FLIGHT (TOF) DETECTORS

- Time-Of-Flight (TOF) method is very effective to detect in "real time" contemporary electrons, protons and ions accelerated in laser-plasma interactions.

TOF technique relies on the measurement of the time needed by a particle to travel for a known distance *d*

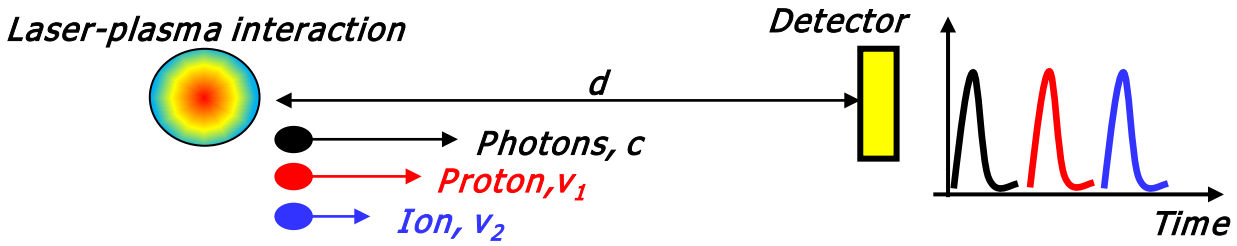

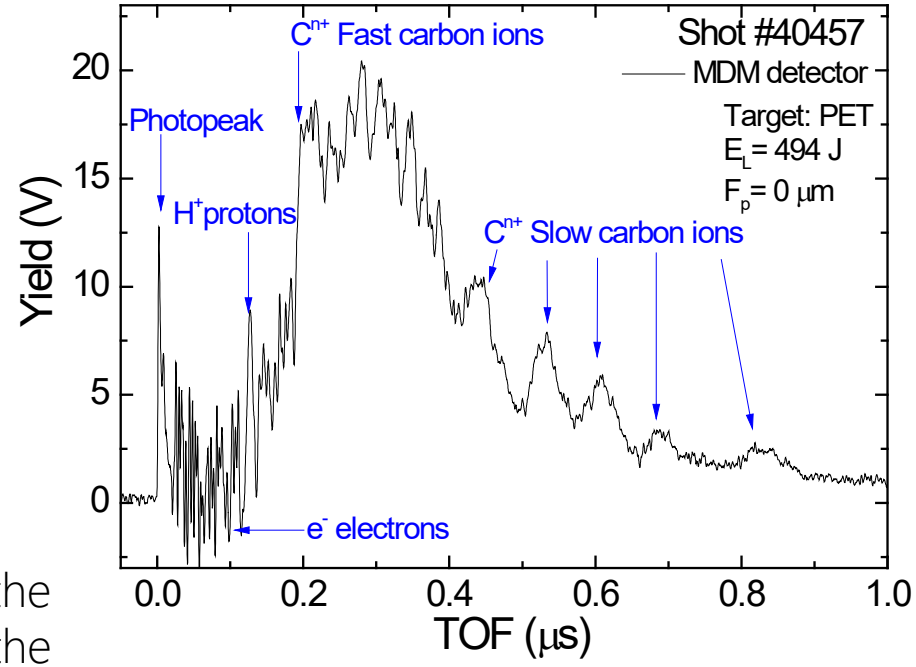

The temporal position t_0 of the photopeak provides a reliable signature of the laser-matter interaction instant. Particle energies are computed evaluating the delay between the signal detection time t_i and t_0.

$$t_0 = t_{pp} - \frac{d}{c} \rightarrow \Delta t = t_i - t_0 \rightarrow v_i = \frac{d}{\Delta t}$$

If the ion mass, *m*, is known, its energy *E* can be retrieved $E = m(\gamma - 1)c^2$

TIME OF FLIGHT (TOF) DETECTORS

Electrostatic detectors

Ion collector or Faraday cups

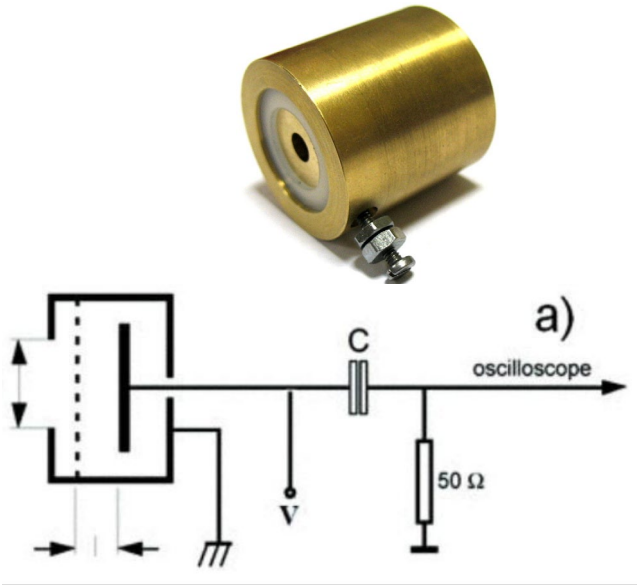

- Small, robustness and reliability compact metallic device designed to catch charged particles in vacuum.
- It consists of two insulated electrodes: the inner electrode is a part of an electric circuit, the outer electrode is grounded and shields the inner electrode from x-rays and scattered particles coming from sides.
- Upon impact of an ion, an electron is drawn from the ground through the current meter to neutralize the positive charge on the inner electrode. Upon impact of an electron, the electron itself travels to the ground and an opposite current is displayed. Charged particle impinging on a metallic surface cause it to gain a small net charge, generating a electric current that can be measured by a fast oscilloscope
- The resulting current can be used to determinate the number of ions or electrons hitting the cup.
- The detectors show low efficiency in detecting low-energy particles and secondary electron emissions can compromise the response of the detector.

TIME OF FLIGHT (TOF) DETECTORS

Scintillators + Vacuum phototubes

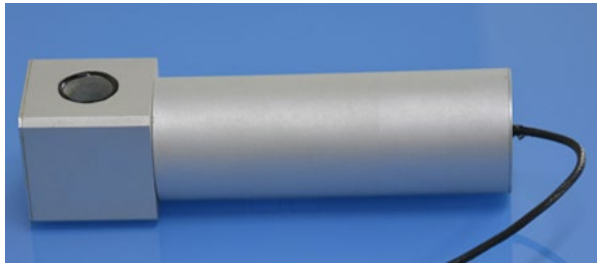

- Scintillator converts the incoming charged and neutral particles in fluorescence light that is then detected by a photo multiplier tube (electric signal).
- Inorganic scintillators have a high light output and a slow response while organic scintillators (crystals, liquids, and plastics) have a low light output but are fast.

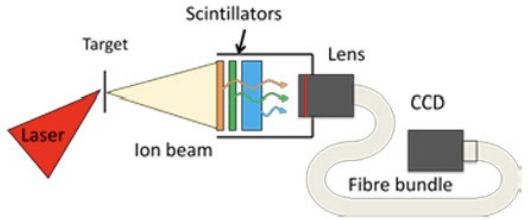

- High efficiency: suitable for low particle fluxes characterized by mid-low energies.
- High energy electrons and x- rays are a potential source of the background signal in the scintillators.

TIME OF FLIGHT (TOF) DETECTORS

Semiconductor devices

- Semiconductor based detectors are devices that use a semiconductor (i.e. Si, GaAs, SiC and diamond) to measure the impinging radiation. Main composition parts of such detectors are active region, constituted by low-doped or intrinsic semiconductor, and junctions located at two sides of the semiconductor.
- Charged particles deposit their energy generating *e-h* pairs that can be collected by applying an external electric field.
- Detection features depend on the semiconductor properties and detector layout.

❑ The different electrodes and geometry layout allow to cover a wide range of requirements

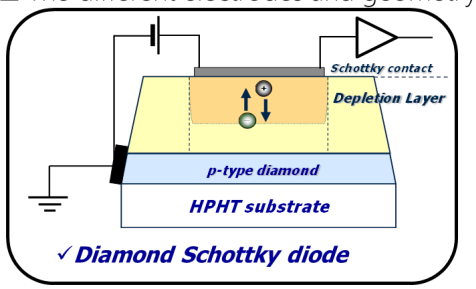

✓ **Diamond Schottky diode**

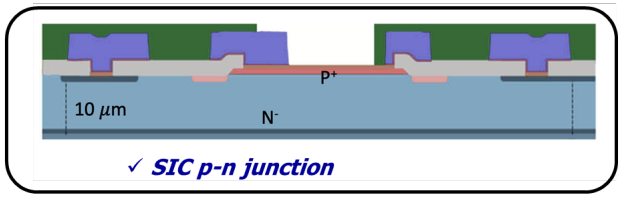

✓ **SIC p-n junction**

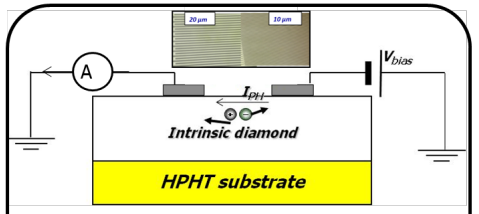

✓ **Diamond with interdigited contacts**

✓ **Metal-Diamond-Metal**

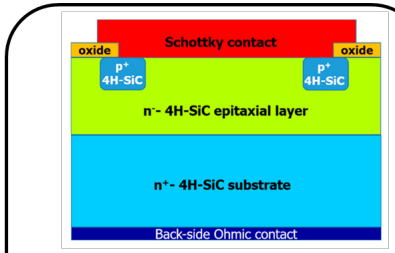

✓ **SIC Schottky diode**

TIME OF FLIGHT (TOF) DETECTOR MATERIALS

	Si	GaAs	4H-SiC	Diamond
	Diamond	Zinc blende	Hexagonal	Cubic
Energy gap (eV)	1.12	1.43	3.26	5.47
Dielectric constant	11.9	12.3	9.7	5.7
Electron mobility ($cm^2/V{\cdot}s$)	1300-1500	8500	800-1000	1800-2200
Hole mobility ($cm^2/V{\cdot}s$)	800-1000	400	100-120	1200-1600
Thermal conductivity ($W/m{\cdot}K$)	145	0.5	370	2290
Hardness (kg/mm^2)	1000	750	3500	10000
Breakdown field (MV/cm)	0.3	0.5	3	>10
Density (g/cm^3)	2.3	5.32	3.1	3.5
Atomic Number Z	14	32	10	6
e-h pair energy (eV)	3.6	4.2	7.8	13
Threshold displacement energy (eV)	13-20	32	25-45	40-50
Max working temperature (°C)	300	450	>1000	>1000

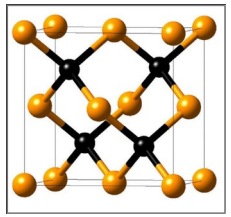

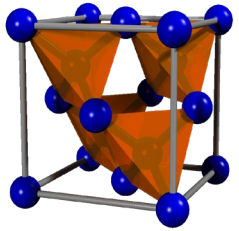

- ✓ VISIBLE BLINDESS (wilde band gap)
- ✓ LOW DARK CURRENT (wilde band gap)
- ✓ FAST RESPONSE TIME (high carrier mobility and low dielectric constact)
- ✓ HIGH RADIATION HARDNEESS (high threshold displacement energy)

Short and narrow photopeak (absolute reference of time measuraments)

Good signal to noise ratio

High energy resolution

TIME OF FLIGHT (TOF) DETECTOR : DIAMOND VS SILICON

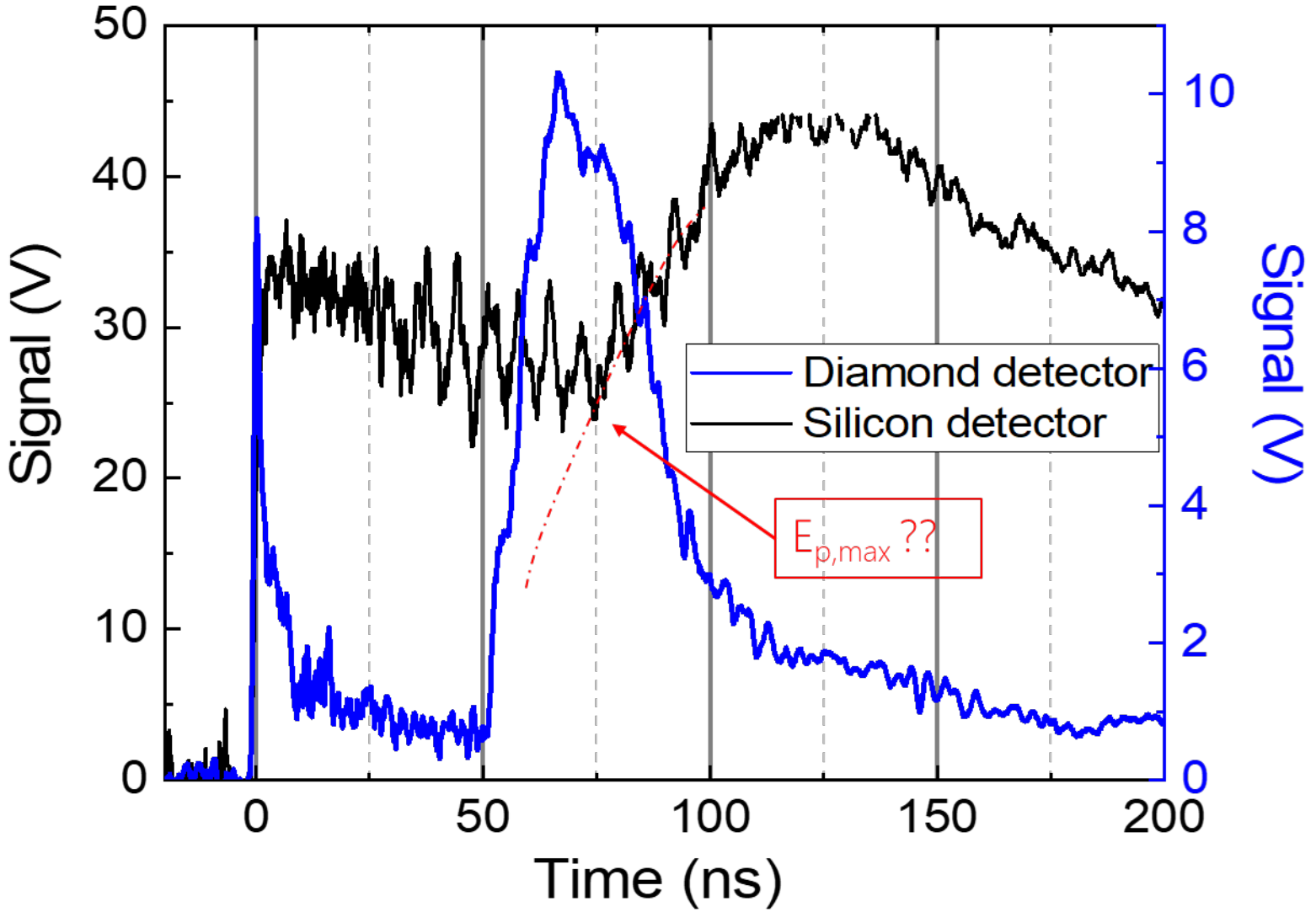

TIME OF FLIGHT (TOF) SEMICONDUCTOR DETECTOR

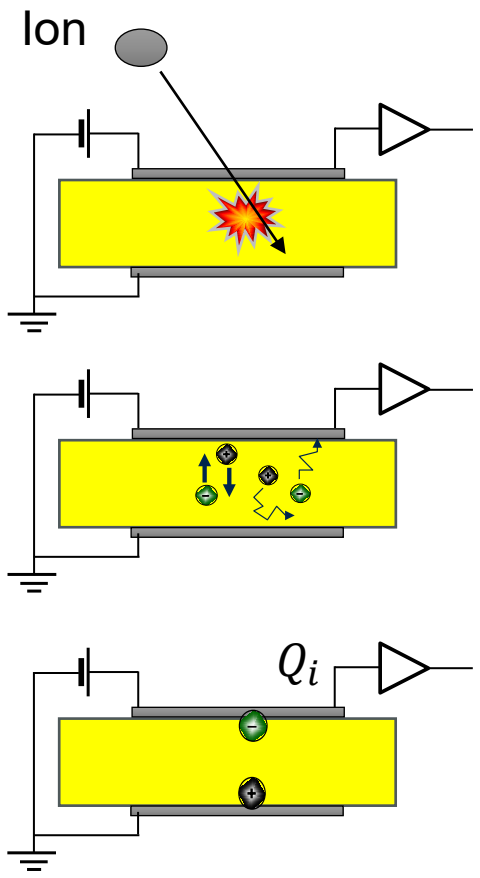

Ions lose their energy dE/dx

If $E_{loss} \geq$ 13.1 eV or 7.8 eV

Production of **free electron-hole pairs**

Charge transport:
1. Drift - in electric field
2. Diffusion

Induced charge Q at sensing electrode

Charge pulse depends on the value of electric field, mobility and lifetime of charge carriers (defects).

$$Q_{i,c} = \boldsymbol{N_i} \frac{\boldsymbol{E_i q_e}}{\epsilon_g} \eta(E_i)$$

$\eta(E_i)$
Charge **C**ollection **E**fficiency

$$N_i = Q_{i,c} \frac{\epsilon_g}{E_i q_e \eta} = \int_0^{t_i} i(t)dt \frac{\epsilon_g}{E_i q_e \eta}$$

From the amplitude of the acquired signal, it is possible to retrieve the number of particles generating it.

Signal generation proportional to the energy deposited by the impinging particles and the number of particles generating it

TIME OF FLIGHT (TOF) SEMICONDUCTOR DETECTOR

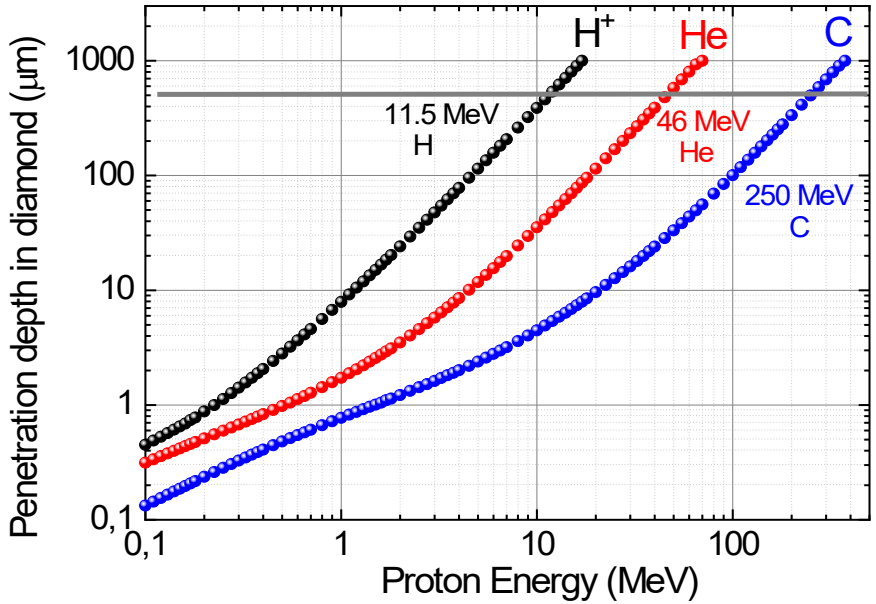

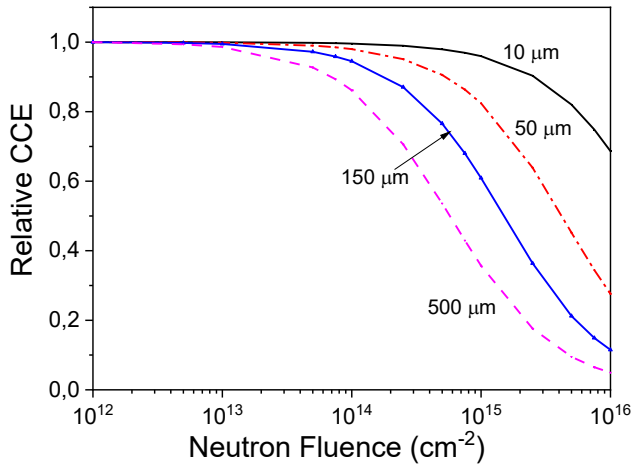

Calculated relative CCE Vs 14 MeV neutron fluence

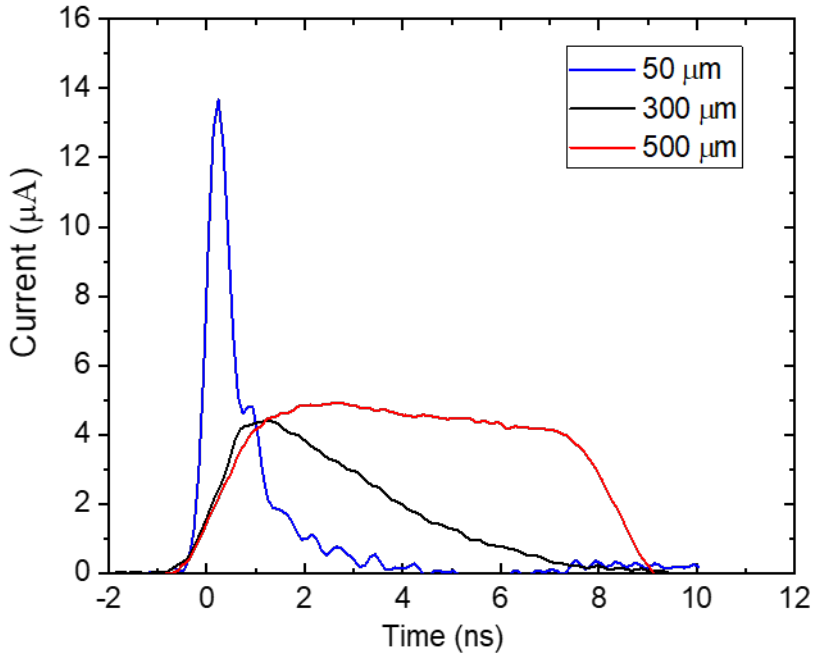

$$\tau_{drift} = \frac{d}{\mu_0 E} \cdot (1 + \frac{\mu_0 E}{v_{sat}})$$

d (distance between electrodes)
μ_0 (electron mobility)
$\boldsymbol{E}$ (electric field)
v_{sat} (saturation velocity)

τ_{drift} depends upon the diamond film thickness and electric field

The **collection time** of the measured pulse can be defined as the time required to the excess carriers to move (drift) toward the electrodes

- Thick detector: High sensitivity, low collection time (low energy resolution), low radiation hardness.
- Thin detector: Low sensitivity, high collection time (high energy resolution), high radiation hardness

TEMPORAL RESOLUTION EFFECT

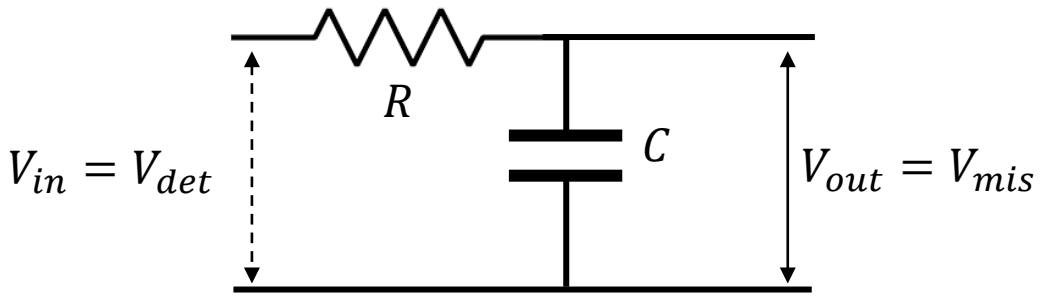

The time response and passive components around the detector can be schematized as a low-pass filter

$$\tau = RC$$

$$V_{out}(t + dt) = \frac{dt}{\tau}[V_i(t) - V_{out}(t)] + V_{out}(t)$$

$Sampling$: $2 \cdot 10^{-10} s$

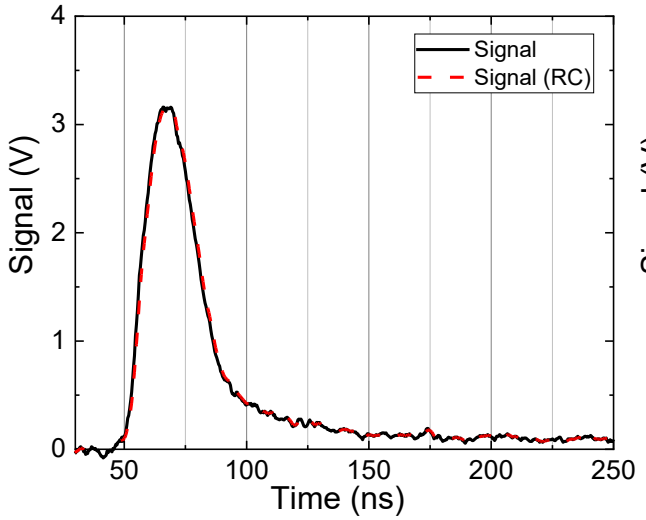

$\tau = 1\ ns$

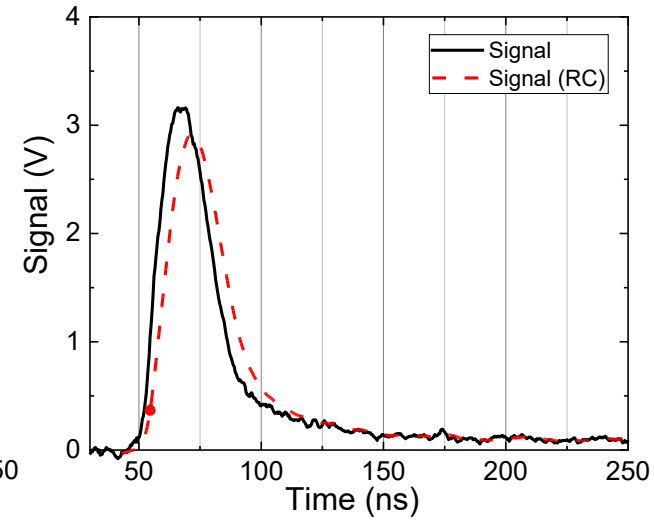

$\tau = 5\ ns$

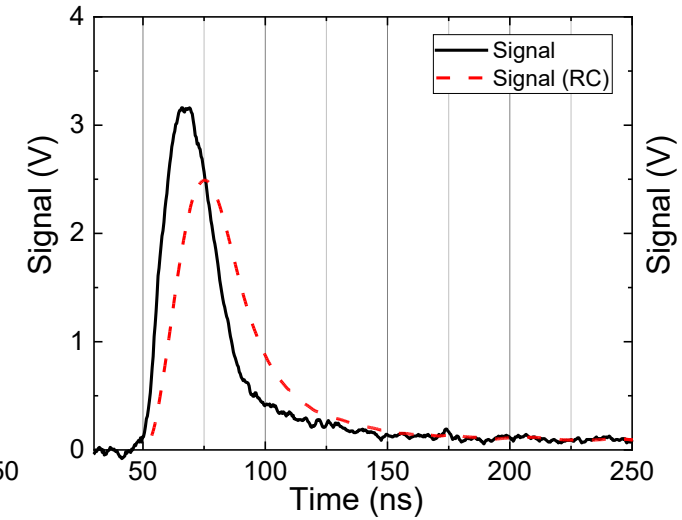

$\tau = 10\ ns$

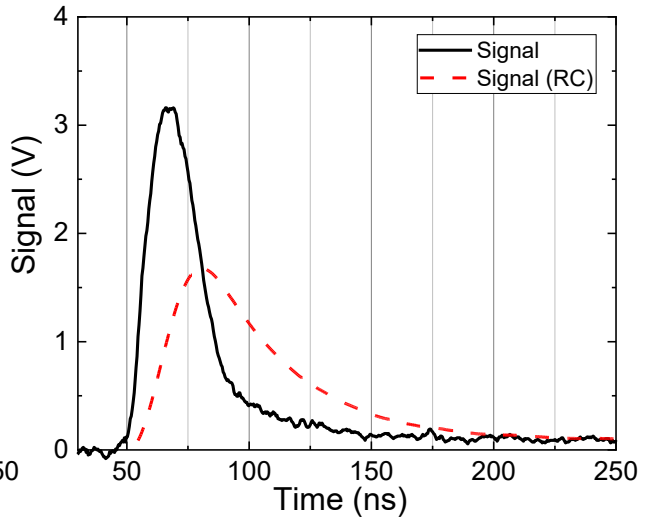

$\tau = 25\ ns$

CHALLENGES IN TOF SIGNAL

Typical signals from **Time Of Flight detector** in Laser-Matter interaction experiments

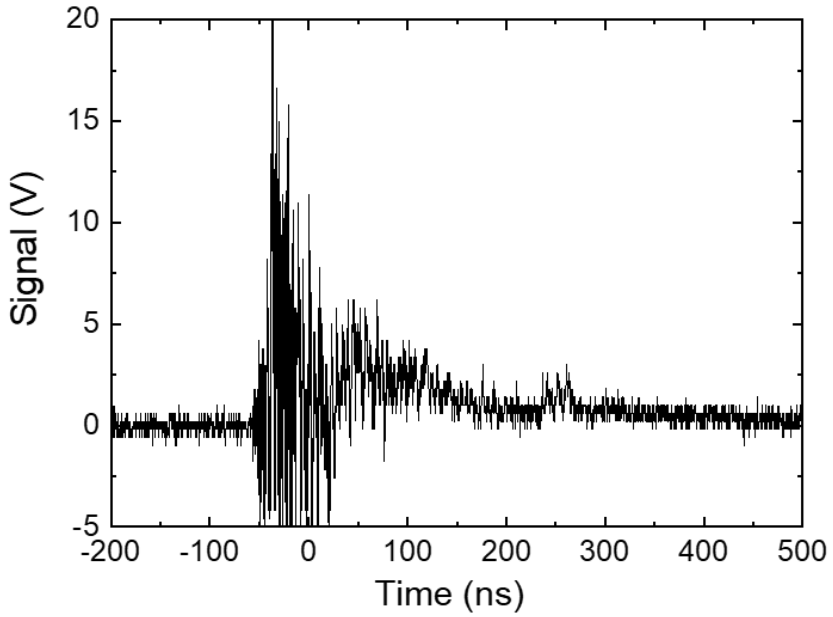

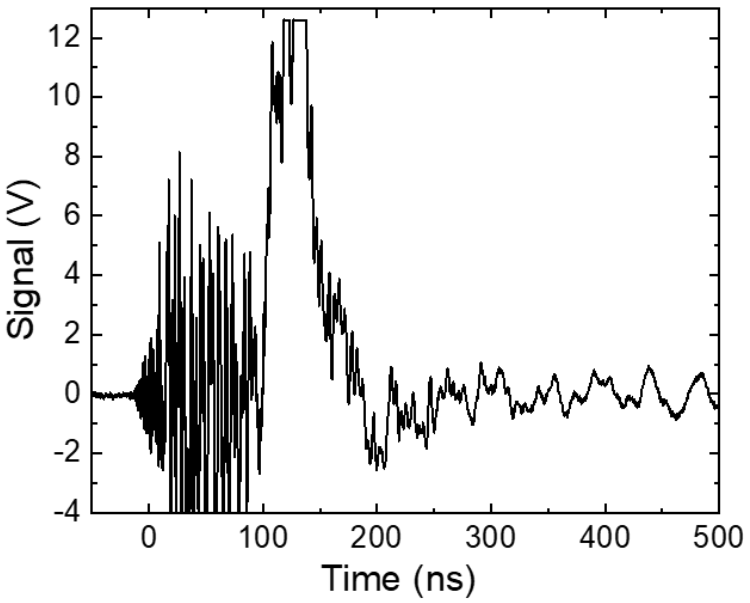

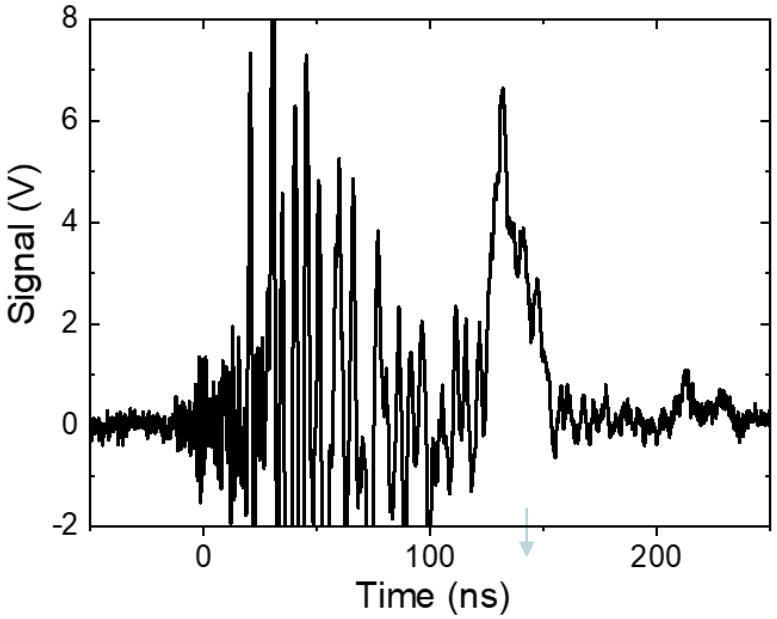

- Low precision in defining t_0 → Poor Energy estimation!
- Bad signal to noise ratio → Poor Energy spectrum reconstruction!

ACQUISITION SYSTEM OPTIMIZATION: EMP MITIGATION

- **EMP pollution** poses a barrier to utilizing TOF detectors in high-energy Laser facilities.

It is necessary to optimize the acquisition system to work in these environments

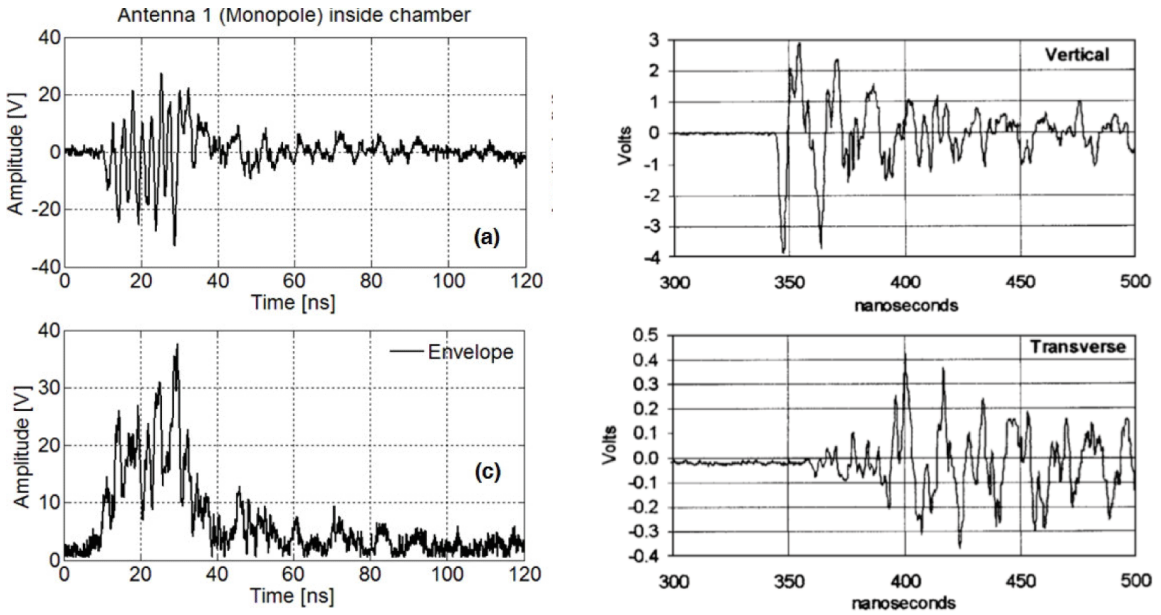

Examples of time-domain signals measured with Antennas inside the vacuum chamber of the ABC and Vulcan facilities

(*F. Consoli* et al, High Power Laser Science and Engineering, (2020), Vol. 8, e22)

t

ACQUISITION SYSTEM OPTIMIZATION: EMP MITIGATION

- **EMP reduction:** TOF detectors are placed in a **proper Al shielding holder** having a pin-hole to collimate the radiation only on the detector sensitive area

EMP attenuation (Skin effect)

$$J_s(z) \propto J_0 e^{-\frac{z}{\delta}} \qquad \delta = \sqrt{\frac{1}{\pi f \sigma \mu}}$$

σ conductivity, μ permeability

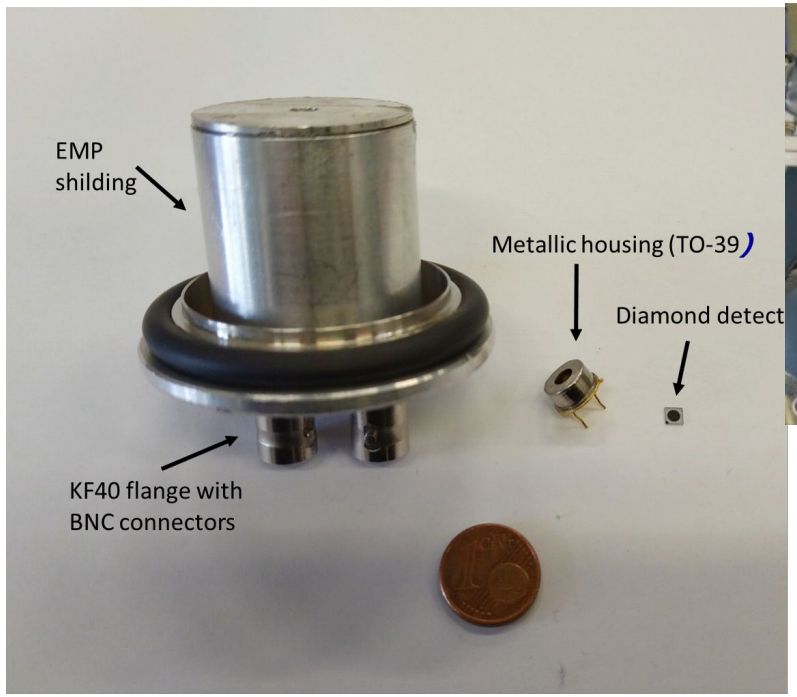

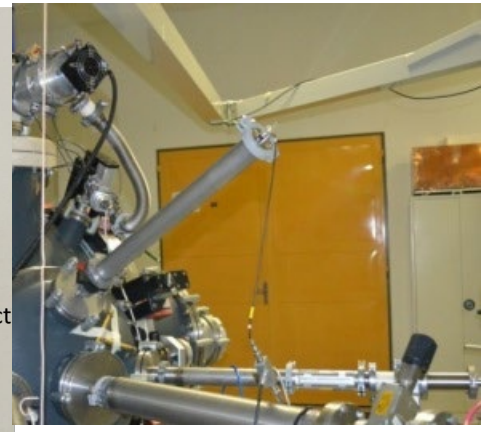

The 3 mm Al thickness can attenuate EMP with frequencies down to 1 KHz

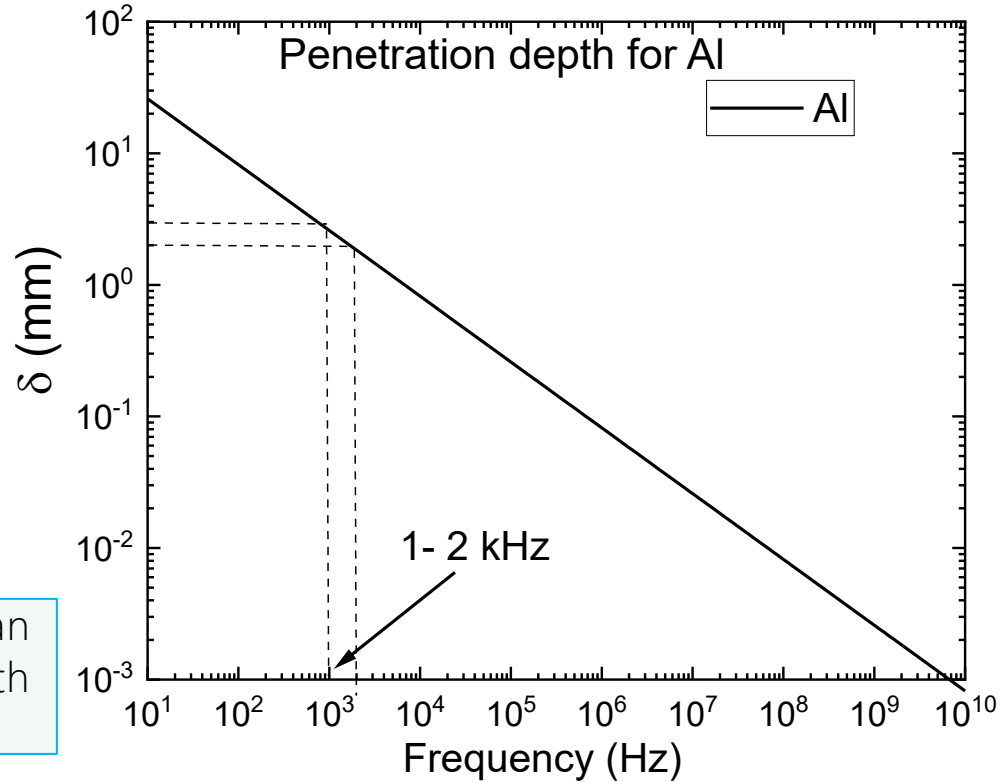

ACQUISITION SYSTEM OPTIMIZATION: EMP MITIGATION

In order to minimize the EMP coupling with the acquisition system and increase the signal/noise ratio, **RG223 or RG214 low noise, double-shielded coaxial cable**s are used.

- **Long double shielded coaxial cables**
  1. Provide **high frequency attenuation (low-pass filter)**
  2. Introduce a **temporal delay (tens of ns) between the TOF signal and the EMP** contribution
  3. Allow to **place the scope far from the experimental chamber**.

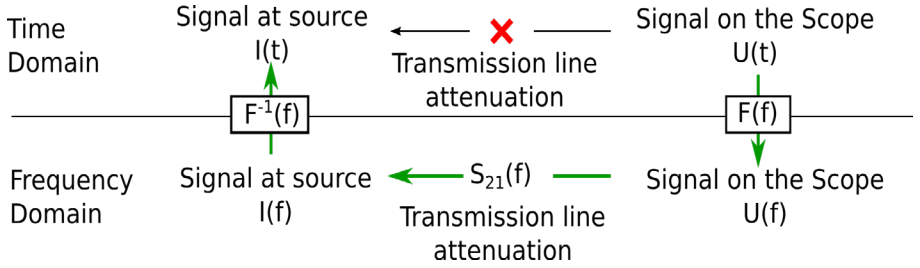

De-embedding procedure $V_D(t) = F^{-1}\left(\frac{F(V(t)}{s_{21}(f)}\right)$

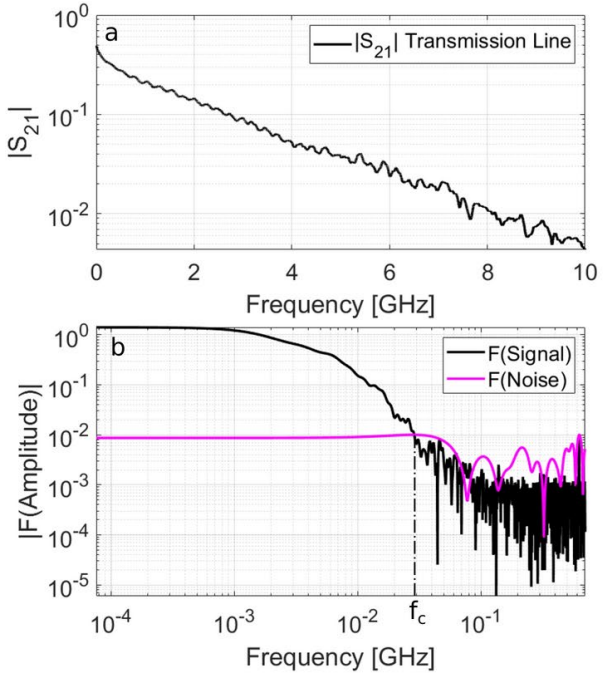

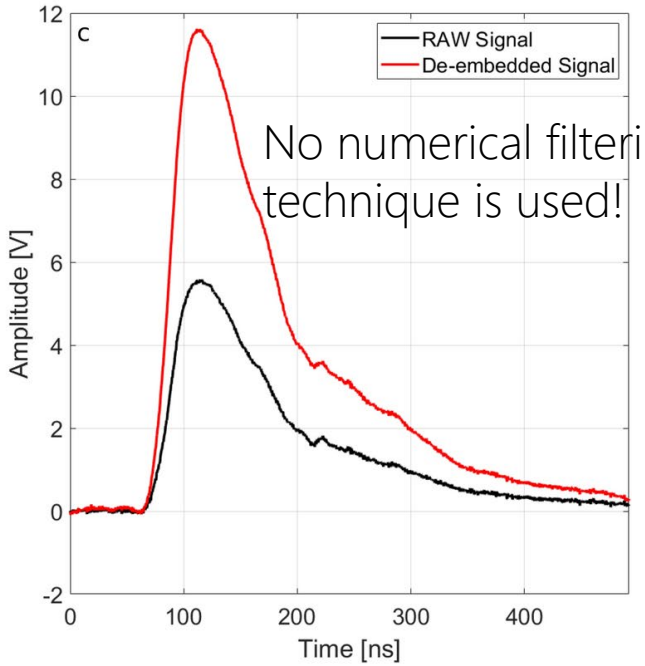

(a) The Scattering parameter S21 of the transmission line (coaxial cables, splitter and bias tee) measured with the Agilent N5230A Network Analyzer (b) Fourier transform of the acquired signal and of the background noise (c) De-embedded signal SD compared with the original raw

M. Salvadori et al. Scientific Reports 11, 3071 (2021)

ACQUISITION SYSTEM OPTIMIZATION: EMP MITIGATION

Typical signals from TOF detector in Laser-Matter interaction experiments after EMP optimization

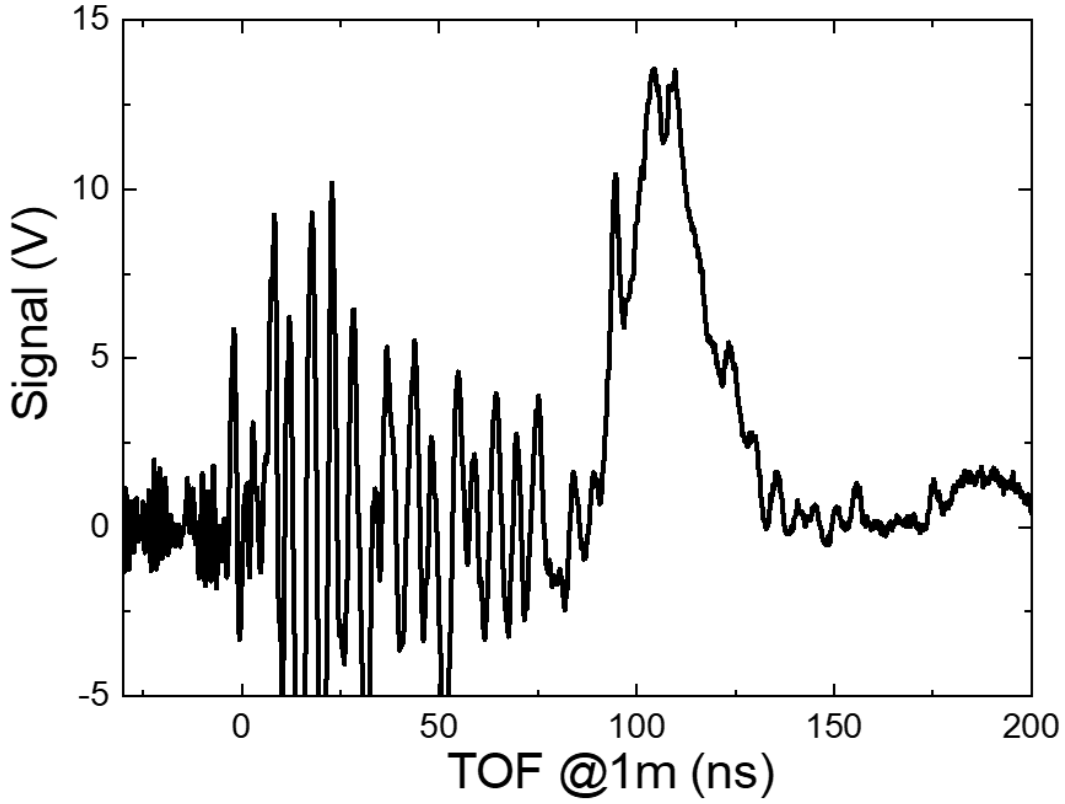

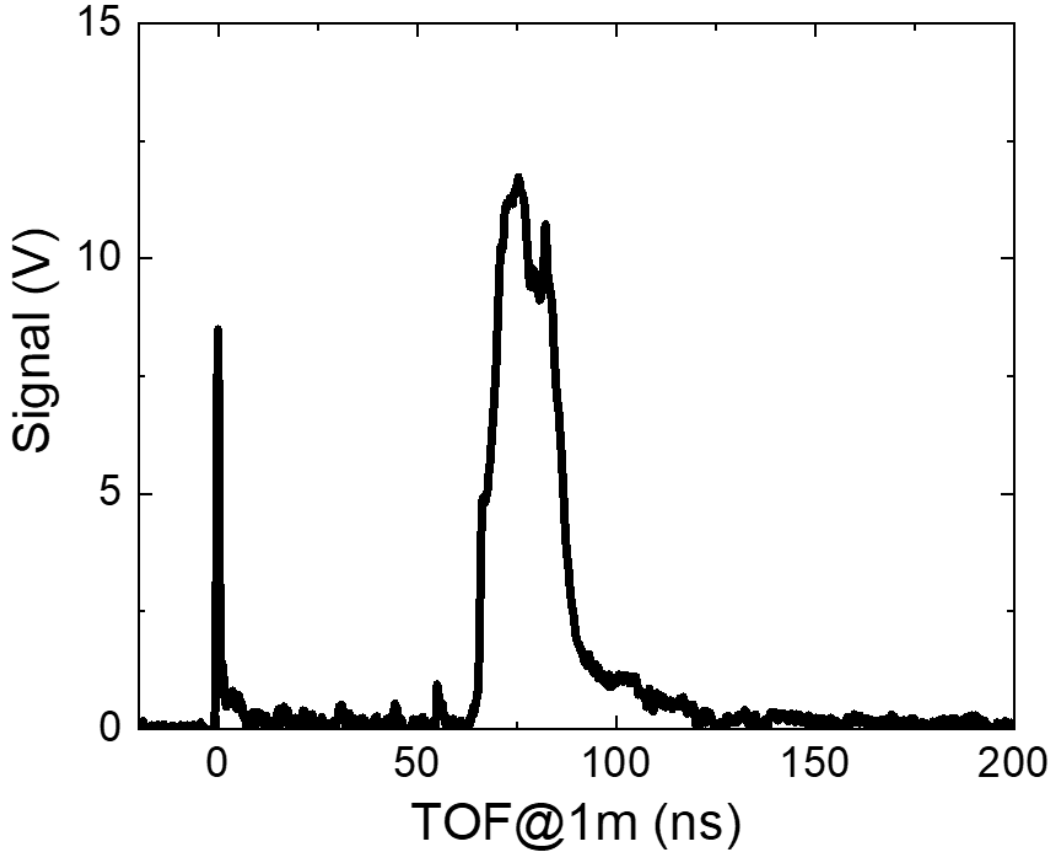

DYNAMIC RANGE ENHANCEMENT

- TOF signals have an intrinsic **high dynamic range**.

It is necessary to develop a technique able to appreciate the full dynamic range

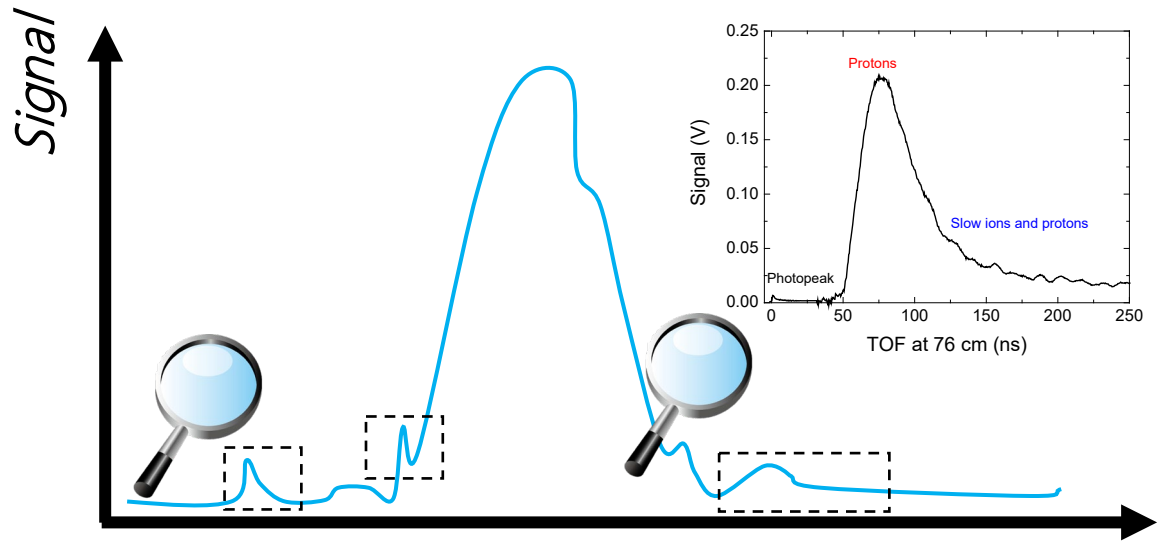

DYNAMIC RANGE ENHANCEMENT

- TOF detectors are connected to fast oscilloscope terminated in 50 Ω though commercial Bias-T.
- **Dynamic range enhancement:** the signal collected from the TOF detector is divided in two parts by a calibrated splitter, both having the same shape but half of the original amplitude. They are acquired by two different channels.

.

Read-out electronics

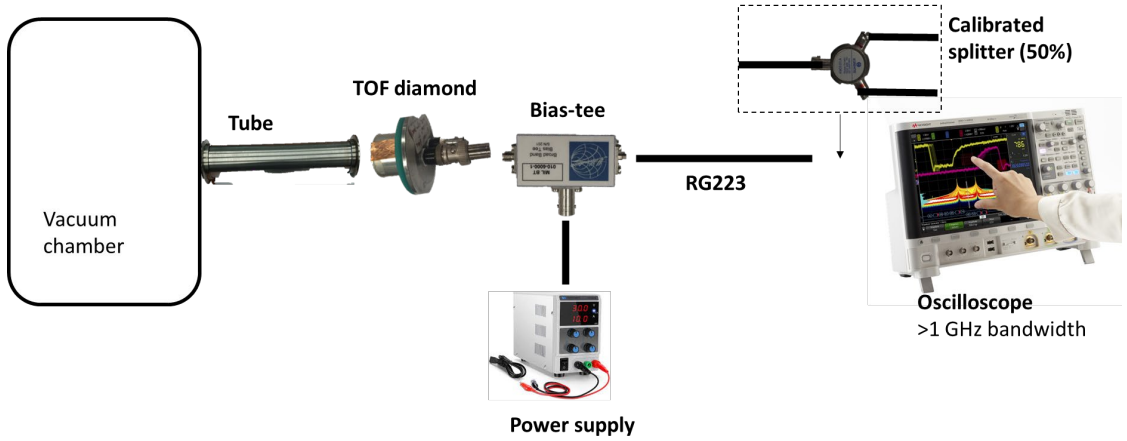

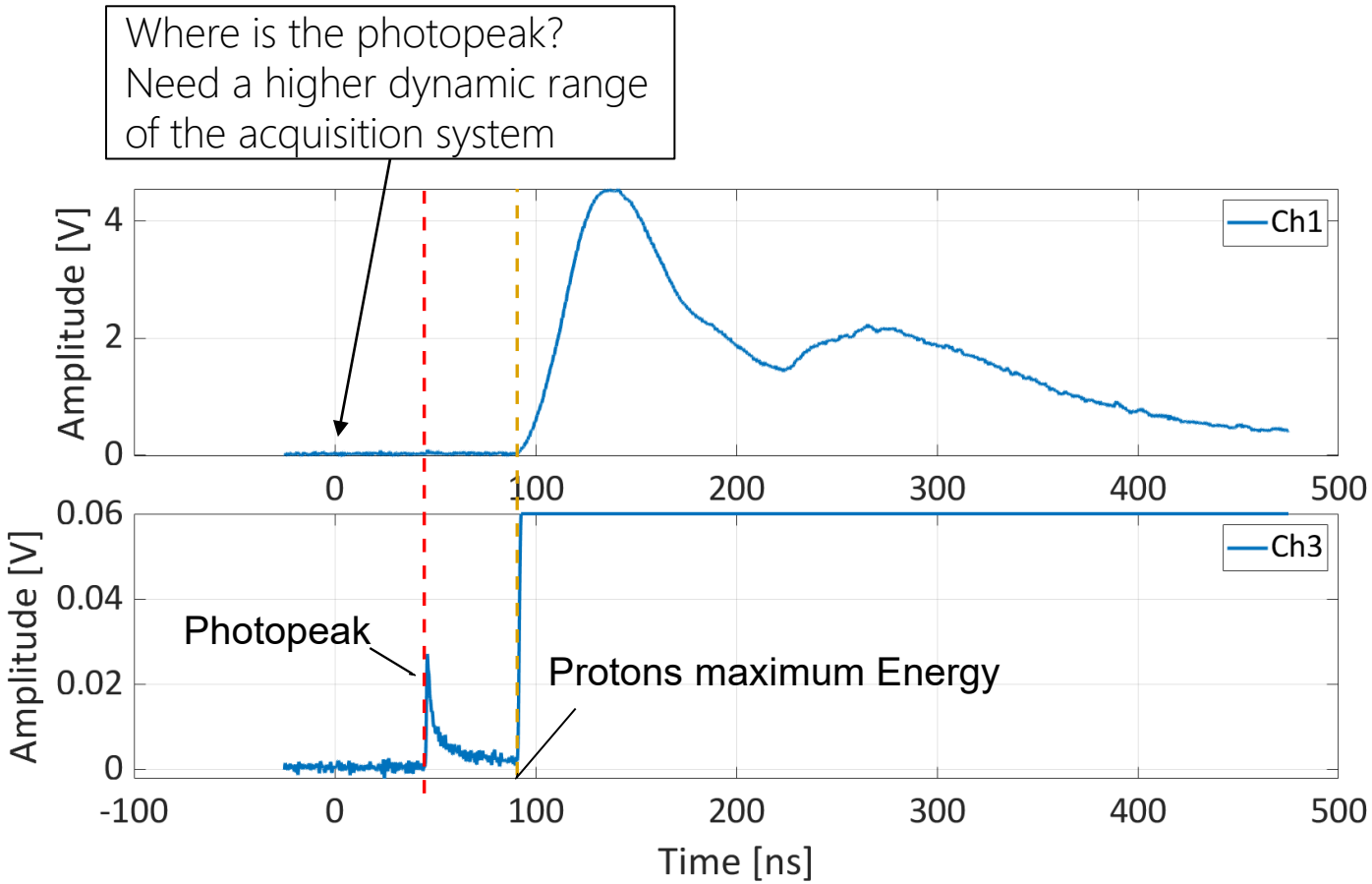

M. Salvadori et al. Scientific Reports 11, 3071 (2021)

THE INGREDIENTS FOR THE SPECTRUM RECONSTRUCTION

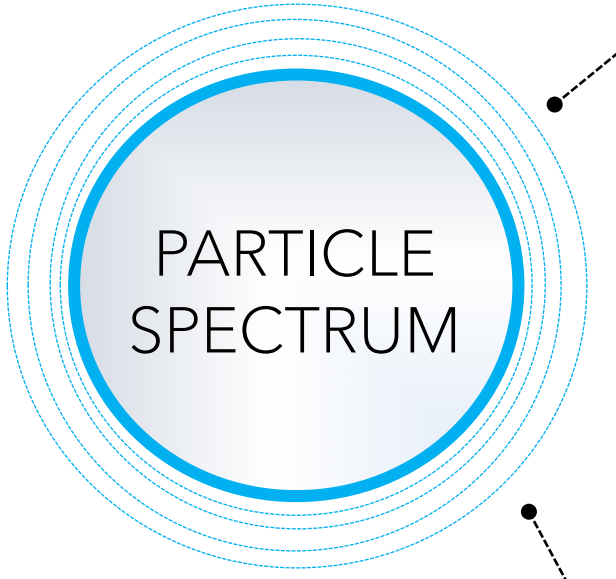

01 SIGNAL ACQUISITION

1. Acquisition and diagnostic system optimization for EMP robustness
2. Enhanced dynamic range

02 ENERGY ESTIMATION

1. Measure the Time-Of-Flight of particles
2. Compute their velocity
3. Retrieve their energy

03 SPECTRUM COMPUTATION

1. Characterization of the Detector used for TOF measurements
2. The energy distribution for a given ion species can be reconstructed from the TOF signal

ANALYTICAL ENERGETIC SPECTRUM COMPUTATION

$$The\ number\ of\ ions\ are\ Q = \frac{q_e N E}{\epsilon_g}$$

$$\frac{dQ}{dt} = i = \frac{q_e}{\epsilon_g}\left(\frac{dN}{dt}E + N\frac{dE}{dt}\right) \approx -\frac{q_e N}{\epsilon_g}\frac{2E}{t}$$

$$N = -\frac{\epsilon_g i t}{2 q_e E}$$

By deriving the *N* respect to the energy, a relation for the signal and the energy distribution can be obtained

$$\frac{dN}{dE} = -\frac{\epsilon_g i t}{2 q_e E^2}$$

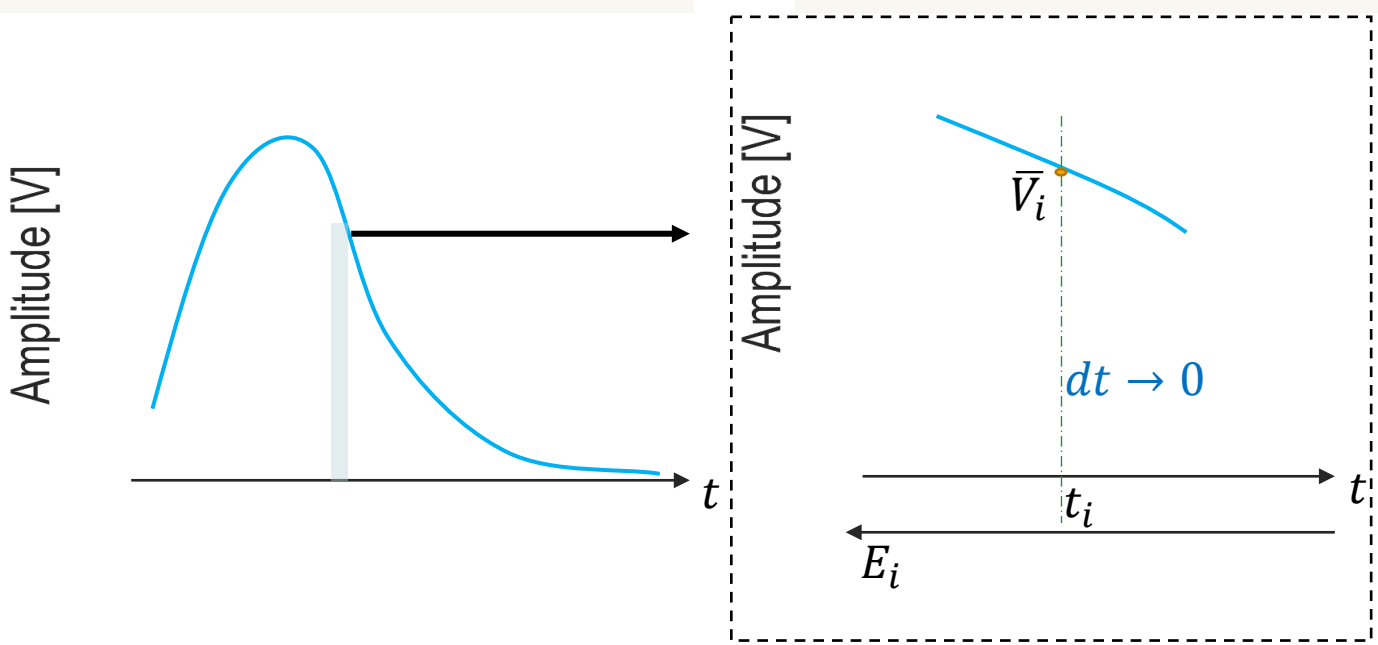

The measured current: $i = \frac{V}{R}, R = 50\ \Omega$ impedence of oscilloscope

Solid angle : $d\Omega = \frac{A}{d^2}, d\ distance\ target - detector, A\ sensitive\ area$

The energy spectrum of particle per solid angle

$$\left|\frac{dN}{d\Omega dE}\right| \cong \frac{\epsilon_g V(t) t d^2}{2 q_e E^2 R A}$$

$$E = m_i(\gamma - 1)c^2$$

$$\gamma = \frac{1}{\sqrt{\left(1 - \frac{\left(\frac{d}{\Delta t}\right)^2}{c^2}\right)}}$$

ANALYTICAL ENERGETIC SPECTRUM COMPUTATION

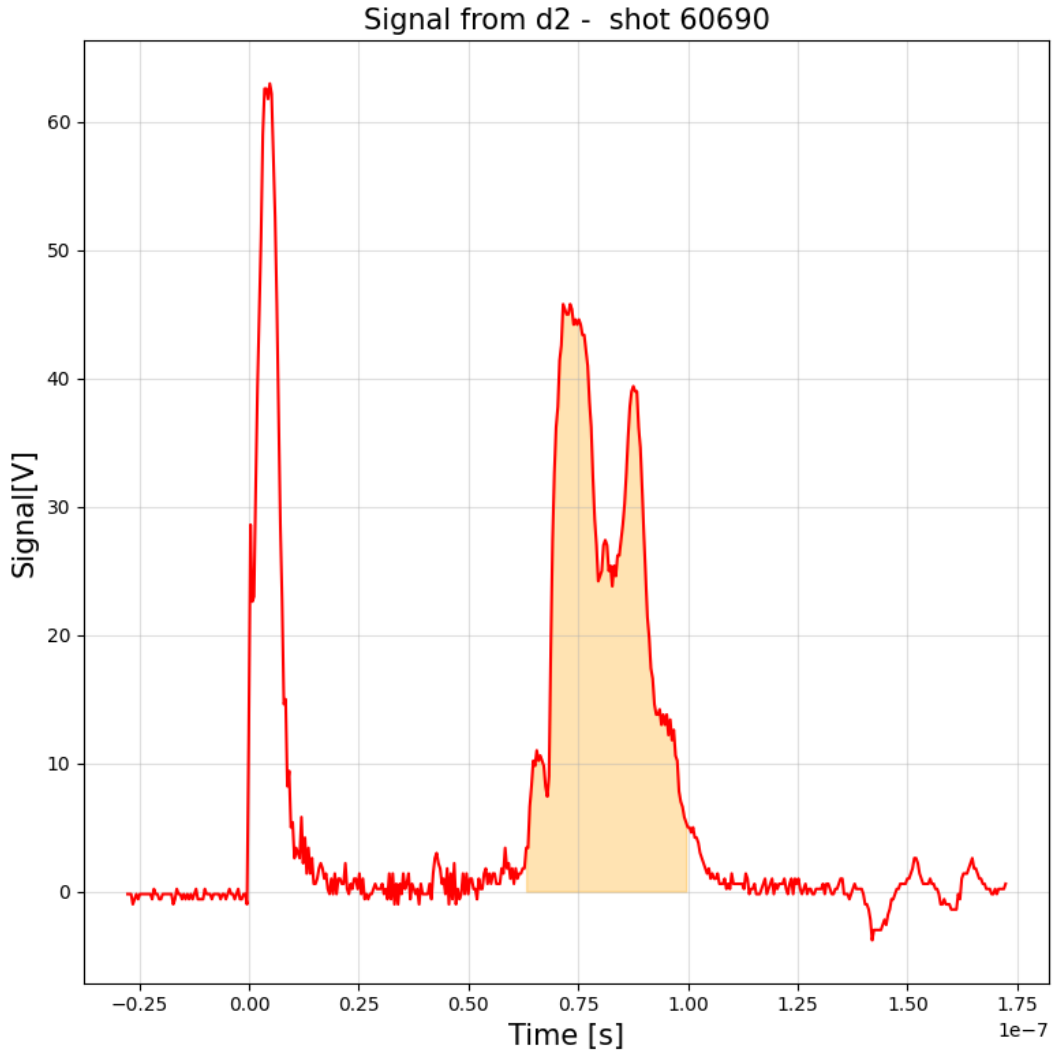

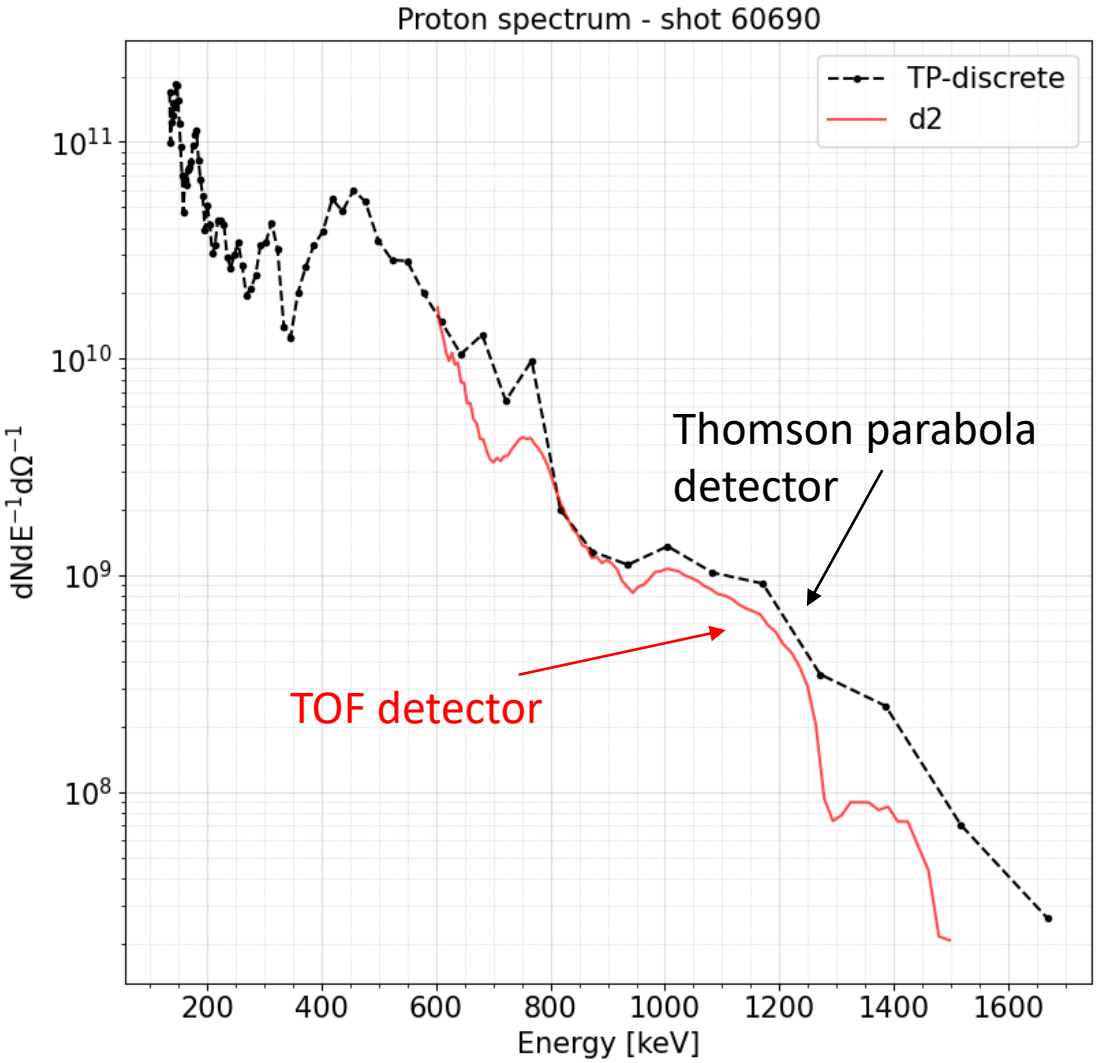

TIME OF FLIGHT (TOF) FOR HIGH ENERGY PROTONS

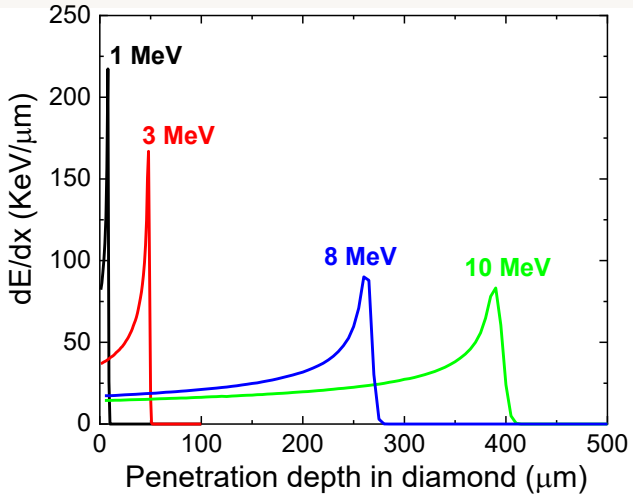

- Laser-accelerated protons having a range less or equal than the detector's active thickness release completely their energy.
- High energy particles (tens of MeV) cross the detector volume, releasing only a portion of their actual energy within it, and the generated charge decreases accordingly.
- The energy estimated through the TOF technique differs from the actual energy released in the detector by the particle.

- A correction factor (*CF*) for energy released (or produced charge) in the detector must be calculated using Geant4 Monte Carlo simulation.

$\boldsymbol{CF} = \mathbf{1}$ the particle is stopped inside the detector: it releases the whole amount of its energy

$\boldsymbol{CF} < \mathbf{1}$ only a portion of the particle energy is released in the active bulk

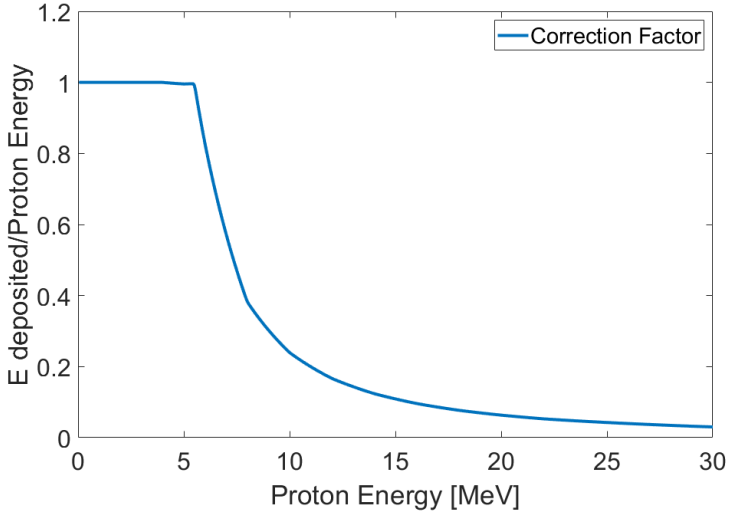

$$Q_{i,c} = N_i \frac{E_i q_e}{\epsilon_g} CF(E_i)$$

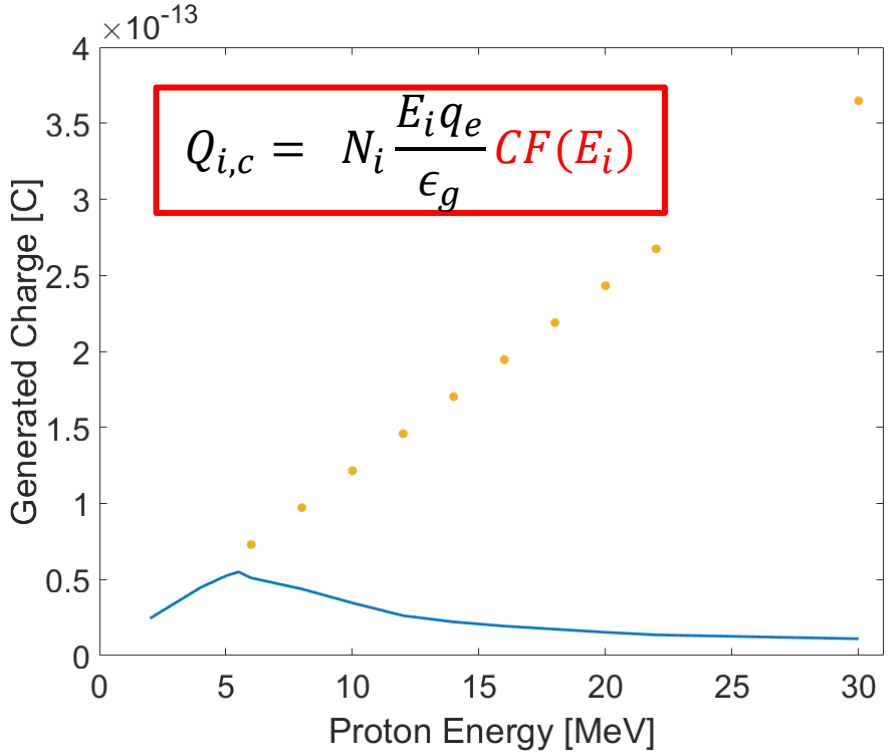

TIME OF FLIGHT (TOF) FOR HIGH ENERGY PROTONS

Protons accelerated by laser-plasma typically present a broad and Maxwellian-like spectrum

$$\frac{dN}{dE} = \frac{N_0}{\sqrt{2Ek_BT}} \exp\left(-\sqrt{\frac{2E}{k_BT}}\right)$$

N_0: Total particle yeald
k_B: Boltzmann constant
T: Plasma temperature

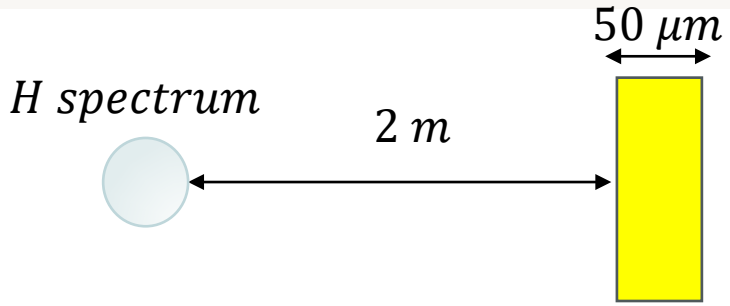

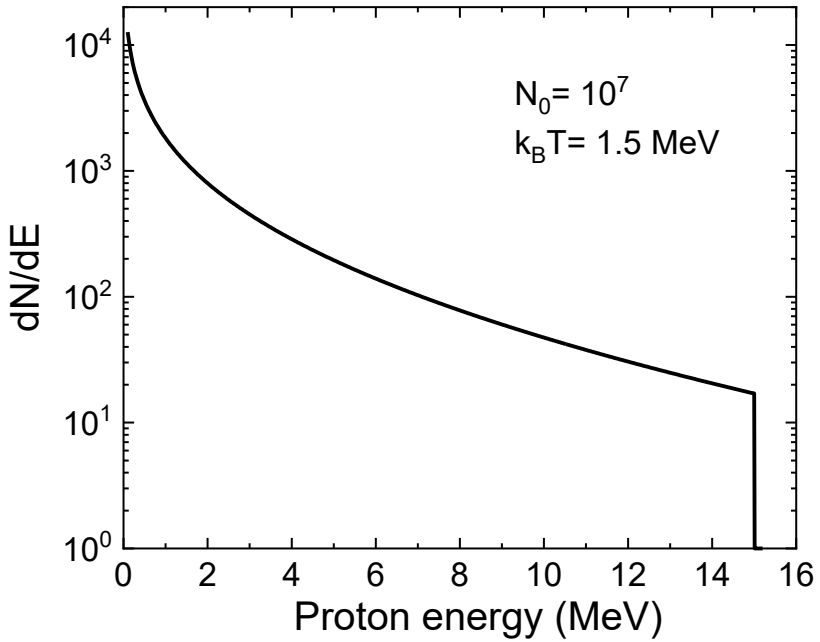

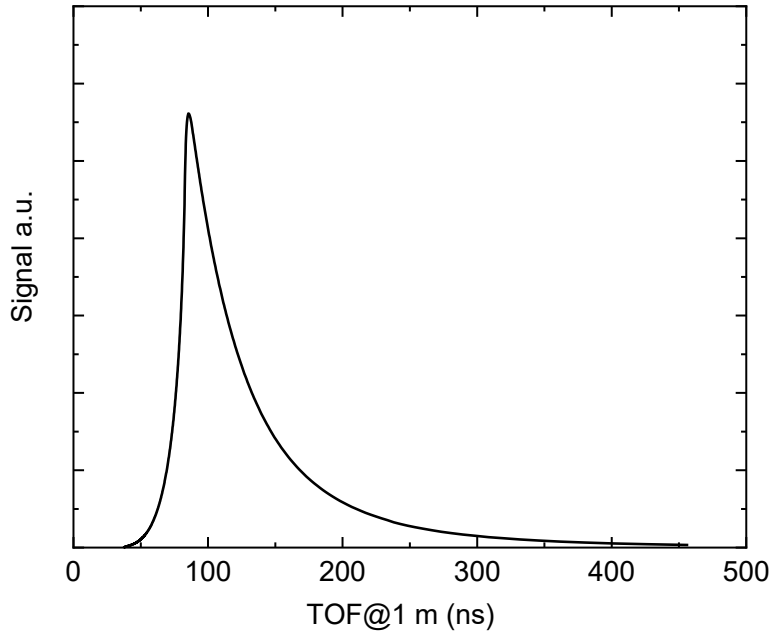

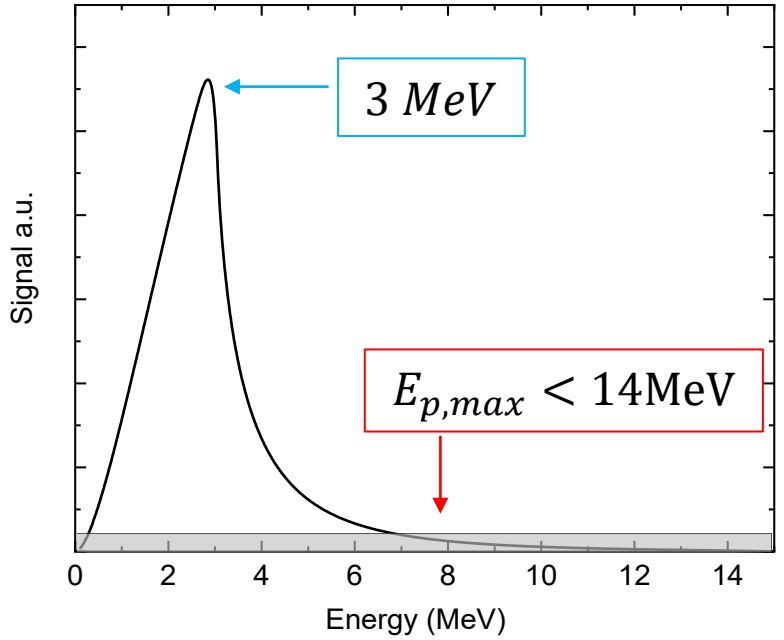

How to overcome this problem?

TELESCOPE CONFIGURATION

- Development of a **telescope detector**: A stack of multiple detectors arranged consecutively along the direction of ions impinging from laser-matter interaction.
- The main advantage of telescope detector lies in the ability to detect high-energy particles with good sensitivity, without compromising energy resolution.
- The use of thin detectors (i.e., 50 μm) could provide high energy resolution and a high radiation hardness for the entire diamond detector.
- The use of a thick detector (i.e. 300 -500 μm) as a stop placed at the end of the telescope is also required.
- The total thickness of the detector is given by the sum of all the detector thicknesses in the stack.

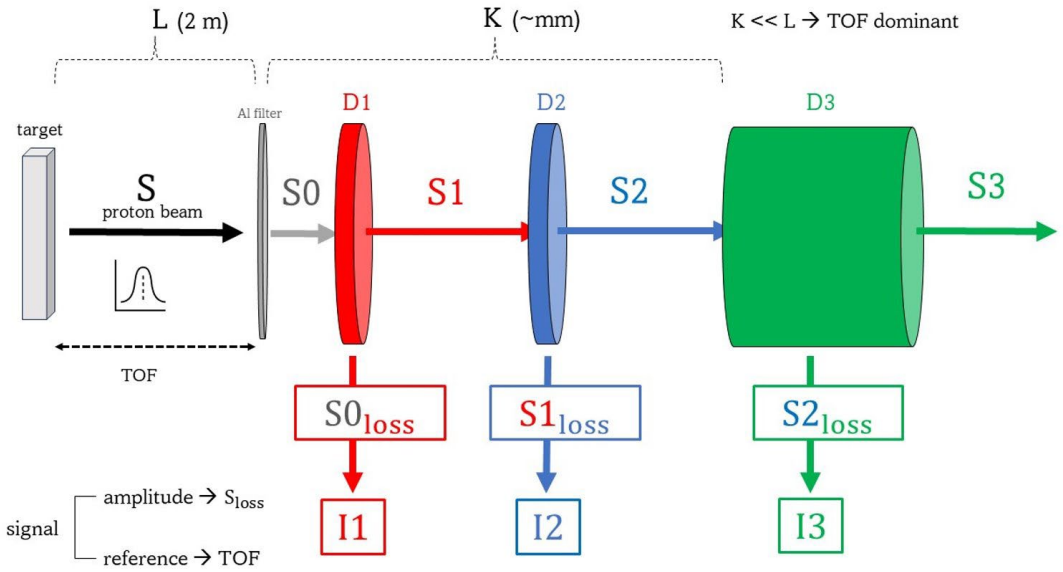

TELESCOPE PROTOTYPE

*Telescope diamond **prototype** consists of three diamonds placed in cascade: 1) 50 micron; 2) 50 micron; 3) 500 μm*

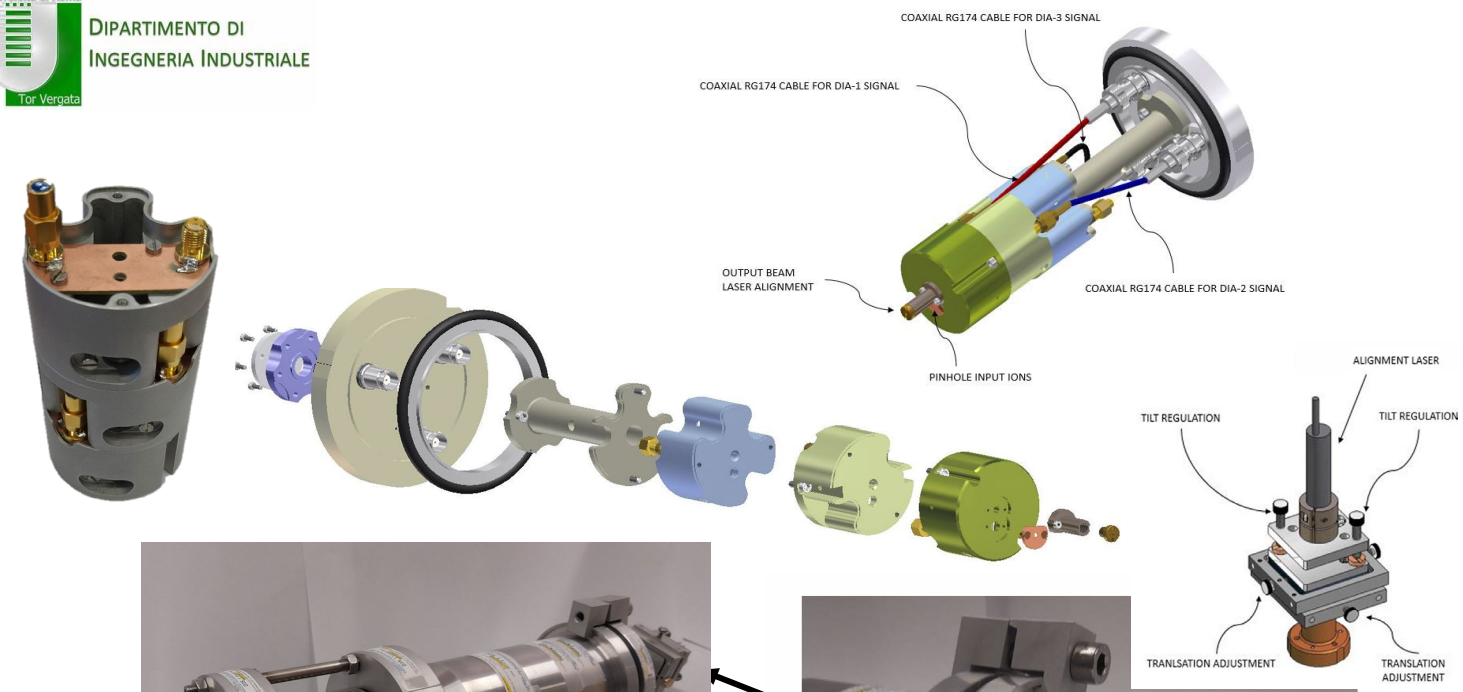

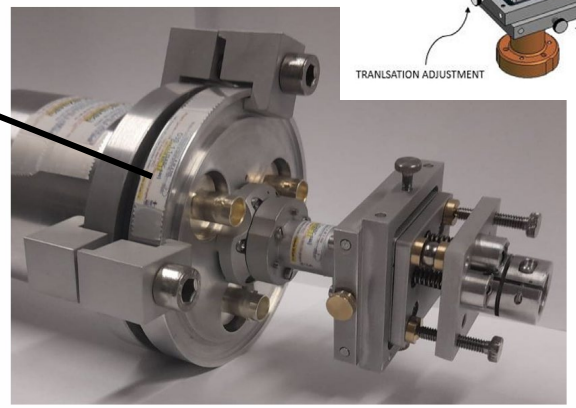

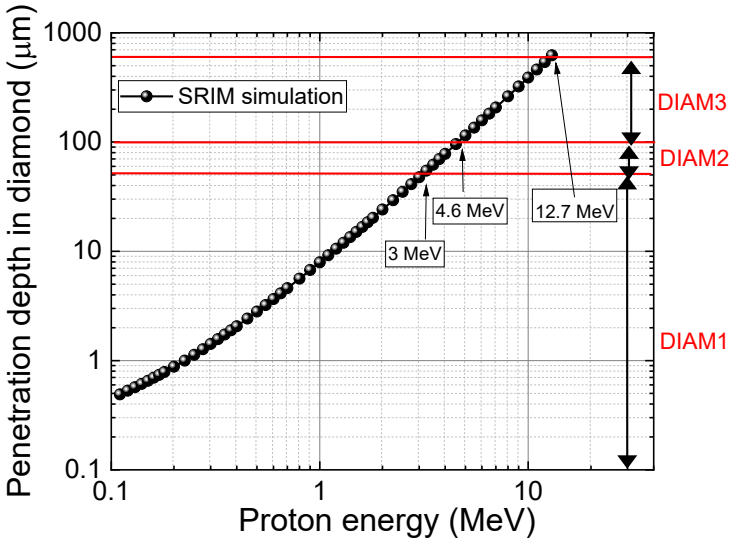

CW laser from a diode is used to align the detector with the interaction point:

- laser alignment is in air, with optical window
- mechanical laser alignment with 3 translations and 3 rotations

TELESCOPE PROTOTYPE

Experimental campaign at CLPU-VEGA III

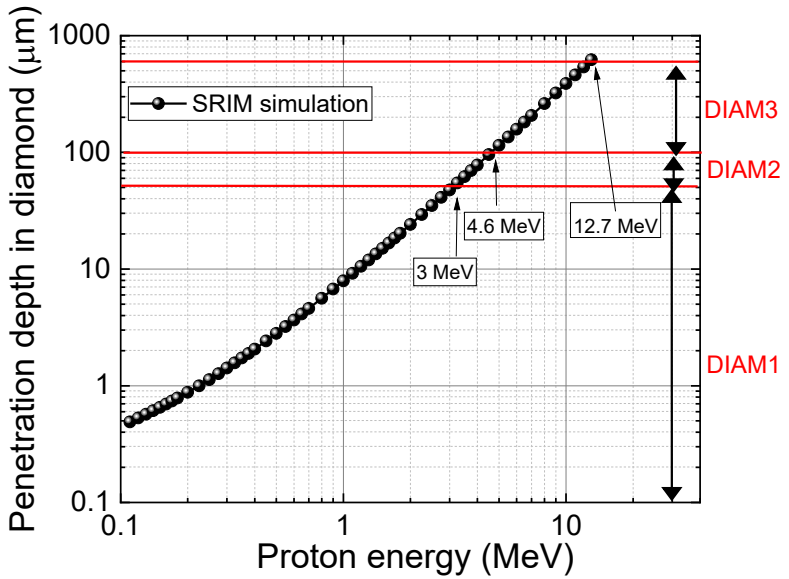

Using this detector, it is possibile to measure high energy of protons (i.e 17 MeV)

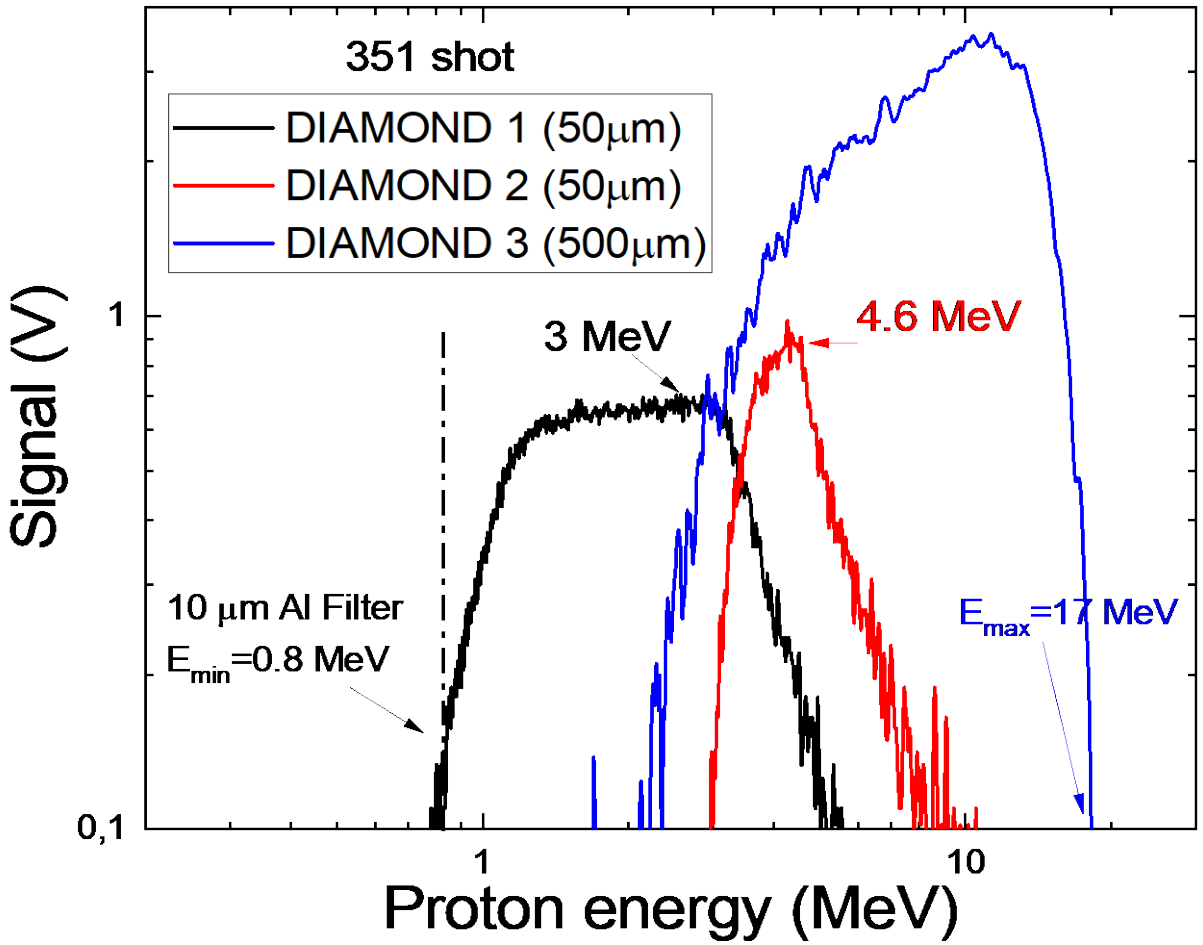

TOF-PARTICLE DISCRIMINATION

- ✓ TOF techniques provide information on particle velocities and the overall energy of ions.
- ✓ TOF metodologies but do not supply information on the particle type.
- ✓ Particles reaching the detector at a given time instant have the same velocity, and thus the same energy per nucleon (Ex. 1 MeV protons or 4 MeV alpha particles or 12 MeV C^{6+}?)

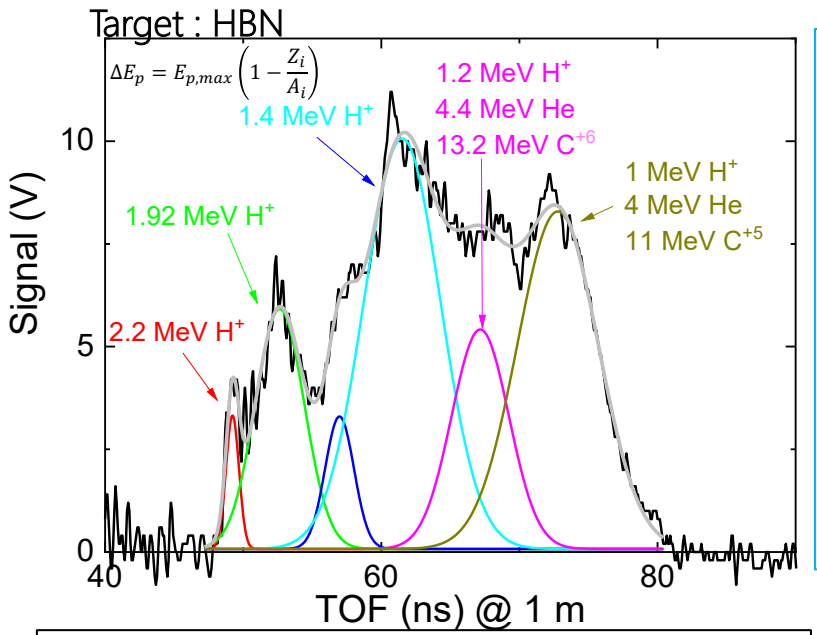

- ➢ Protons, occurring at 49 ns TOF indicate that they have the maximum kinetic energy at 2.2 MeV.
- ➢ The proton energy range is ($E_{p,max}/2$, $E_{p,max}$) where no contribution coming from the superimposition of other ions.
- ➢ The ion acceleration produced by the charge plasma separation in the TNSA regime is of about 2.2 MeV per charge state (Coulomb–Boltzmann–Shifted (CBS)-like distribution).
- ➢ Ion energy distributions are shifted toward the higher energy in proportion to their charge state (ex. 13.2 MeV C^{6+} , 11 MeV C^{5+})
- ➢ In $p^{11}B$ fusion experiment, alpha particles (He) centered at about 4 MeV can be also produced.

10 μm Al filter	-14.5 μm in Al @ 1 MeV H -15.8 μm in Al @ 4 MeV He - 9.3 μm in Al @ 11 MeV C -11.2 μm in Al @ 13.2 MeV C

How to overcome this problem?

- ➢ The use of an array of detectors, nominally identical, featuring different calibrated foil filters of different thicknesses to exploit the different stopping powers of ions of different species and energies.

TOF-PARTICLE DISCRIMINATION

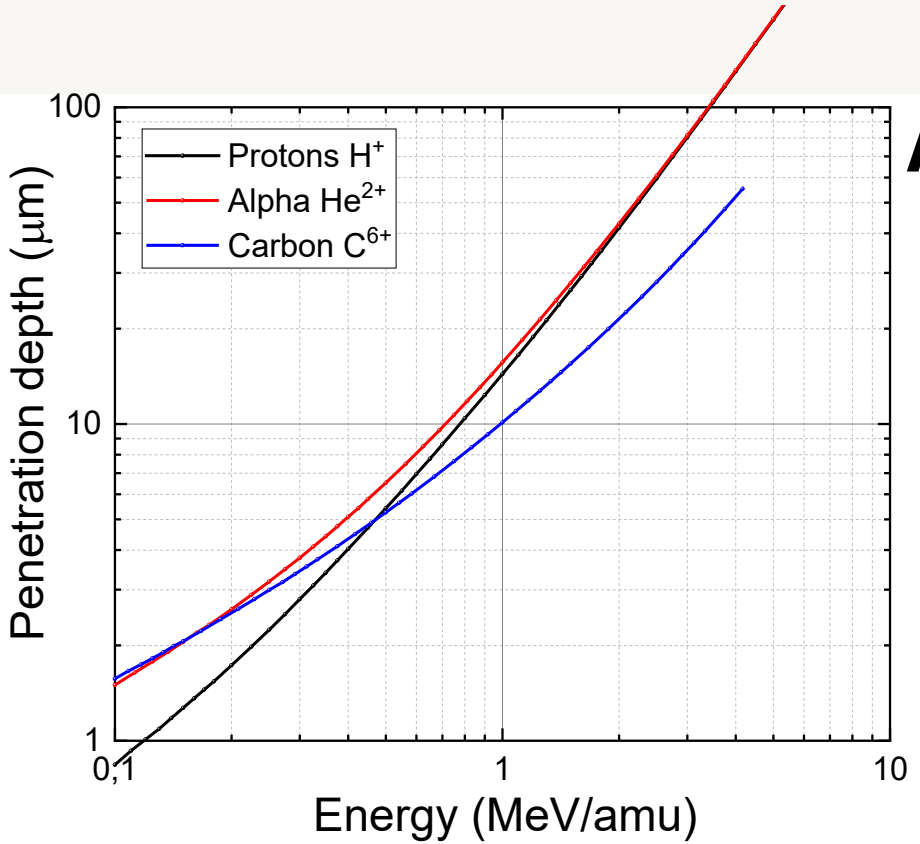

Al filter

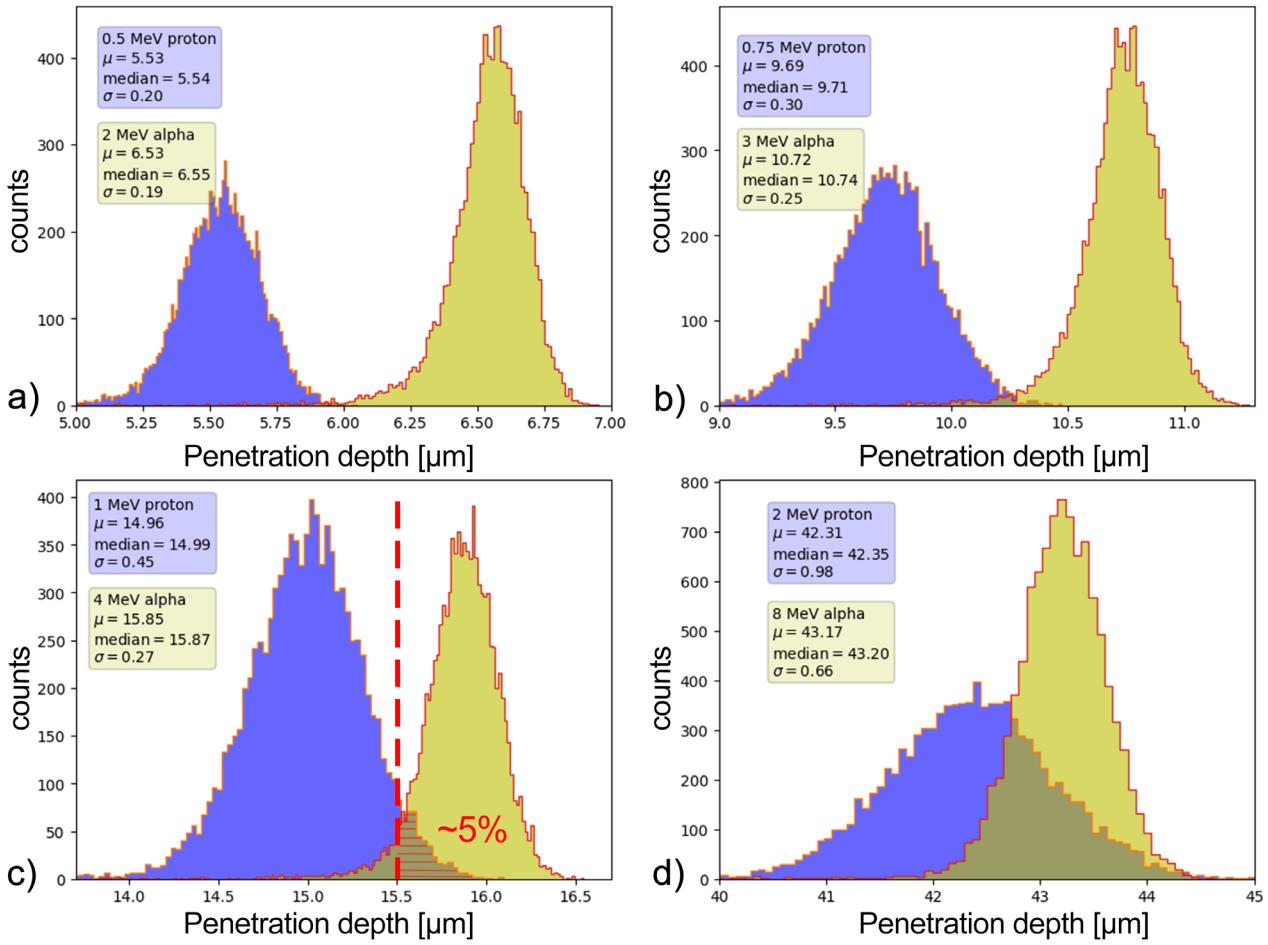

- Particle discrimination is not possible for each energy and ion specie.
- At low energies: discrimination difficult for alpha and carbon ions but ok for protons. At high energies (>1.5 MeV/amu): no discrimination is possible between protons and alphas but ok for the carbon ions.
- The choice for the thickness and material for each filter can vary depending on the species to be discriminated.

TOF-PARTICLE DISCRIMINATION

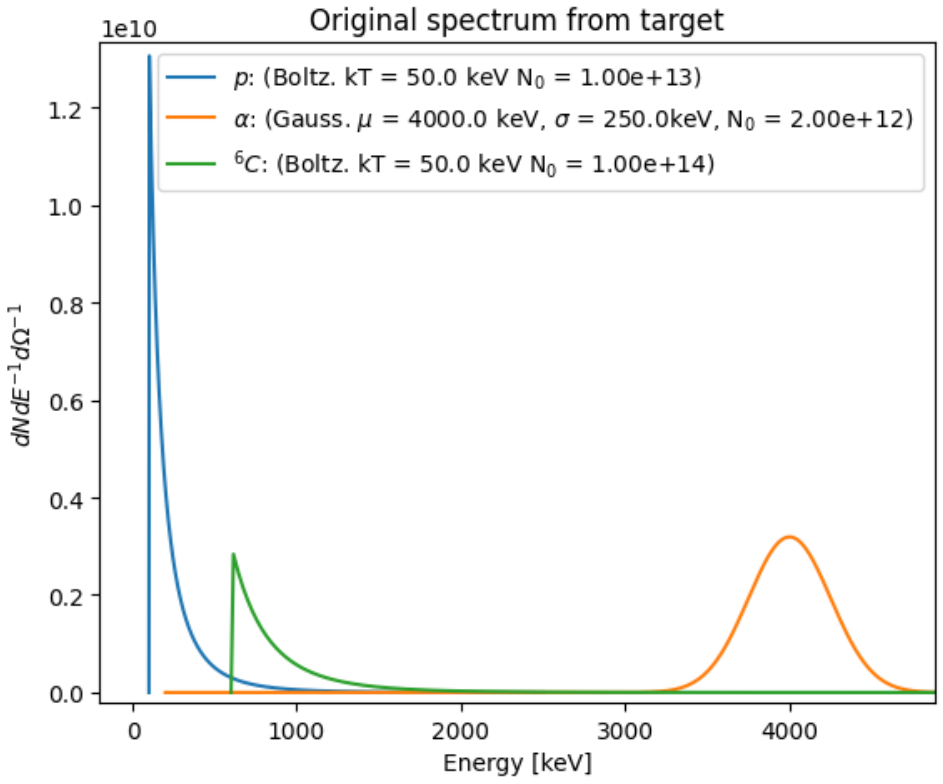

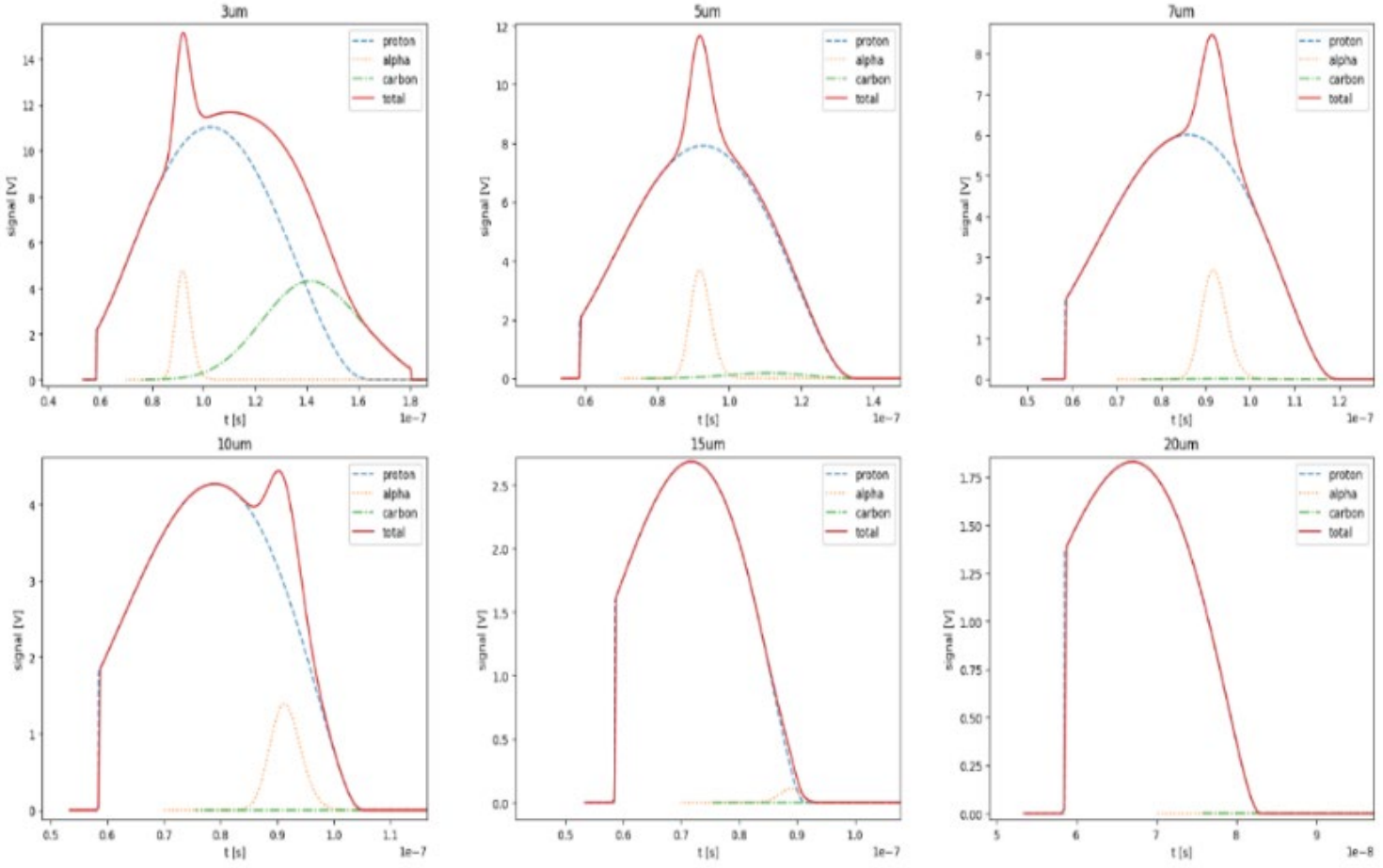

0.1 – 2.5 MeV for H (Boltzmann distribution)

0.6 – 14 MeV for ^{6}C (Boltzmann distribution)

4±0.5 MeV for He (Gauss distribution)

ARRAY DETECTOR FOR PARTICLE DISCRIMINATION

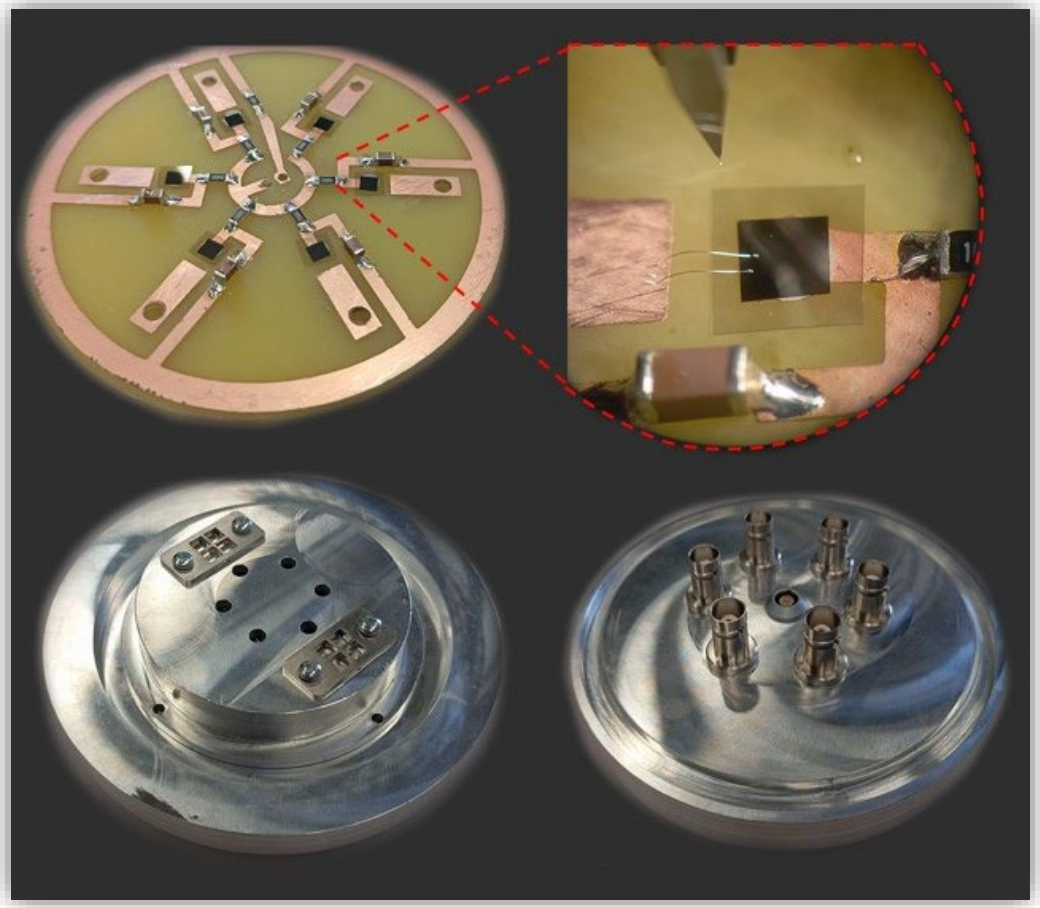

- Six TOF diamond detectors with the same geometric characteristics (sensitive volume: 35 μm in thickness and 15 mm^2 area) arranged in an array configuration with Al filters.
- Thanks to the different stopping powers of particles of different mass and energy within the filters it becomes possible to obtain more information about the respective particle energy spectrum.
- Two CR39 plates with the same filters are placed next to diamonds for comparison the results.

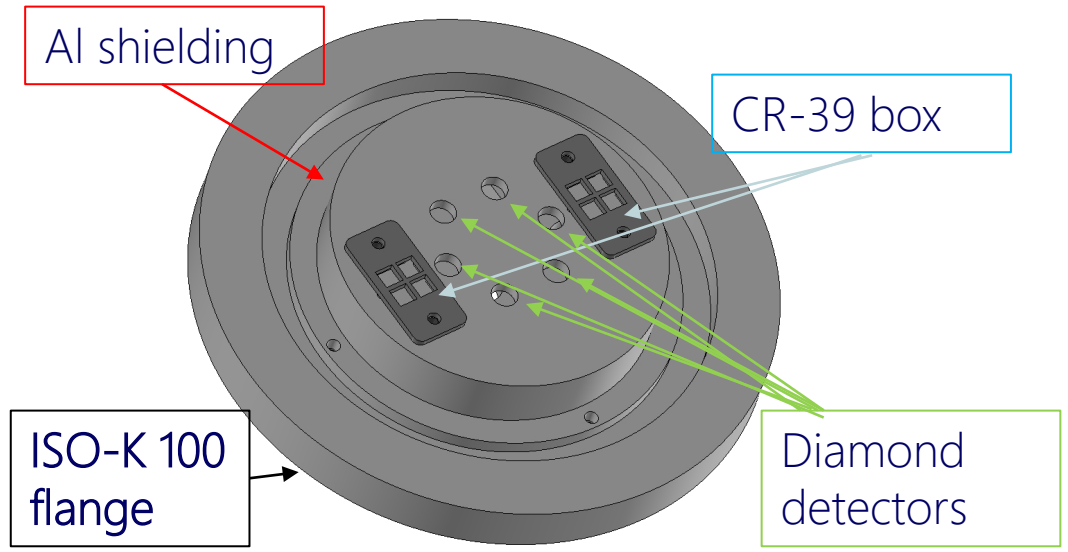

ARRAY DETECTOR FOR PARTICLE DISCRIMINATION

METHODOLOGY

1. We start with an assumption of laser-driven ion emission spectra distribution (Boltzmann Distribution for H, C and other ions, Gaussian distribution for He).
2. We employ Monte Carlo simulation to precisely track the energy loss of ions (H, He, C, etc.) as they traverse through the Al filters.
3. Subsequently, we generate a calculated ion distribution impacting the detector for any given ion at any given energy.
4. The altered ion distribution after passing through the filters modifies the amplitude of the signals (y-scale), while the Time of Flight (TOF) (x-scale) is correlated with the energies of ion emission spectra.
5. We then calculate the combined signals generated in the detector and compare them to the measured signals.
6. Using convergence methods, ion spectra parameters that best ft the measurements can be selected.
7. The results are compared and completed with that obtained by CR39 detectors.

THANK YOU FOR LISTENING

Claudio Verona

claudio.verona@uniroma2.it